

To determine the sensitivity of the new method, Munc13-4-deficient platelets were mixed with normal platelets at varying ratios. Western blot analysis could not detect Munc13-4-deficient platelets easily, even when the proportion of normal platelets was as low as 25% (Figure 4D). In contrast, flow cytometric analysis easily identified 10% Munc13-4-deficient platelets among 90% normal platelets (Figure 4D), which proved the high sensitivity of the method in diagnosing FHL3.

## Discussion

FHL is a rare but life-threatening inherited immune disorder for which mutations in 4 genes have been identified as causative factors. *PRF1* encodes the cytolytic effector protein perforin that forms a pore-like structure in the target cell membrane.<sup>1,12</sup> A mutation in *PRF1* results in FHL2,<sup>7</sup> which accounts for 20%-50% of FHL cases.<sup>4,5</sup> *UNC13D* encodes the protein Munc13-4, which is crucial for the fusion of cytolytic granules to the plasma membrane and the subsequent release of perforin and granzymes.<sup>1,12</sup> Mutations in *UNC13D* result in FHL3,<sup>8</sup> which accounts for 20%-30% of FHL cases.<sup>4,12</sup> FHL4 is caused by mutations in *STX11*, which encodes syntaxin-11.<sup>9</sup> Mutations in *STXBP2*, which encodes Munc18-2, were recently reported to cause FHL5.<sup>10,11</sup> Syntaxin-11 and Munc18-2 also mediate the fusion of cytolytic granules to the plasma membrane.<sup>1,5,12</sup> The ability to screen for FHL2-5 rapidly would facilitate the initiation of life-saving immunosuppressive therapy and the preparation of FHL patients for hematopoietic stem cell transplantation.

In the present study, we found that the Munc13-4 protein is expressed abundantly in platelets (Figure 1A-B). The detection of Munc13-4 protein in platelets by Western blotting (Figure 1C) or flow cytometry (Figure 4A-B) was a reliable screening method to identify FHL3 patients. Munc13-4-deficient platelets were identified easily among normal transfused platelets by flow cytometry, which indicated that this method could be applied to patients who are receiving platelet transfusions during the acute phase of the disease (P5 in Figure 4A). Detection of intraplatelet Munc13-4 was enabled by the use of highly specific antibodies against the full-length human Munc13-4 (supplemental Figure 1).

There is a possibility that FHL3 patients with residual Munc13-4 protein expression could be overlooked by the screening methods described in this study. Most FHL3 patients have mutations that result in the absence or significant reduction of Munc13-4 protein expression,<sup>16,23</sup> as was the case with the patients screened in this study (Figure 1C), which suggests that the mutated Munc13-4 protein is unstable. The NK-cell degranulation assay, which was performed for every referred sample with a sufficient number of NK cells, revealed defective degranulation only in the identified FHL3 patients (date not shown). These results indicate that the majority of mutations in *UNC13D* are likely amenable to rapid detection by the new methods described in this study. Comparative studies on the *UNC13D* genotype, Munc13-4 protein expression, and the lysosomal exocytosis assay must be performed to confirm the reliability of these methods.

It was also investigated whether the analysis of lysosomal release by platelets could be used as an alternative method to screen for FHL3. Profound impairment of lysosomal exocytosis by platelets during the acute phase of the disease and restoration of this impairment after clinical remission was observed in FHL3 and in some secondary HLH patients (Figure 3). It is not clear whether

this transient impairment of platelet degranulation is involved in HLH pathogenesis or if it merely reflects in vivo platelet activation by diffuse endothelial damage during the acute phase of the disease that renders them unresponsive to ex vivo stimulation. The release of lysosomal granules by Munc13-4-deficient platelets was impaired only minimally at steady state (Figure 3A and 3C), which is in contrast to a recent study showing the involvement of the Munc13-4 protein in the release of lysosomal granules in mouse platelets.<sup>27</sup> Although the precise reason for this discrepancy is unclear, platelet degranulation is likely to be regulated differentially between species; for example, Munc13-4-deficient mice have bruising and bleeding tendencies<sup>27</sup> that are not commonly associated with human FHL3. Further studies are warranted to elucidate the exocytosis pathways of platelets and their role in the pathophysiology of HLH.

With the development of tools for rapid screening, the diagnostic approach for FHL has changed over the years. Impaired NK cytotoxicity was the first reported signature clinical finding of FHL patients.<sup>13,14</sup> Defective CTL activity was subsequently reported as another hallmark of FHL.<sup>7,8,16,28</sup> However, NK-cell activity is also decreased in some cases of secondary HLH,<sup>15,17-20</sup> and the CTL cytotoxicity assay is not readily accessible to most clinicians. The NK-cell lysosomal exocytosis assay is a comprehensive method to identify patients with a degranulation defect.<sup>10,11,22-24</sup> However, this analysis is not available in some patients with extremely reduced NK-cell numbers, which are often observed during the acute phase of HLH.<sup>19</sup> Although CTLs can be an alternative tool to perform the lysosomal exocytosis assay,<sup>24,28,29</sup> it remains impossible to differentiate FHL3-FHL5.<sup>10,11,23,24</sup> Impairment in these assays warrants the genetic confirmation of FHL, but sequencing all of the candidate genes is not a suitable approach for rapid diagnosis. Flow cytometric detection of perforin expression in NK cells is a reliable and rapid way of identifying patients with FHL2,<sup>21</sup> and the new method described in this study for the detection of Munc13-4 expression in platelets would add to the rapid diagnosis of FHL3.

Platelets could also be used for the screening of FHL4 and FHL5 because they share some granule-transport mechanisms with other types of hematopoietic cells, including CTLs and NK cells.<sup>2,30,31</sup> Indeed, in the present study, both syntaxin-11 and Munc18-2 were expressed abundantly in platelets (data not shown). We are currently using platelet proteins to screen for FHL4-FHL5 by Western blot analysis, although no cases have been found so far because of the extreme rarity of these disorders.

In summary, platelets abundantly express Munc13-4 protein and are a useful tool to screen for FHL3. By detecting intraplatelet Munc13-4 expression by flow cytometry, it is now possible to rapidly screen for FHL3 with a very small sample of whole blood, even in the acute disease phase requiring platelet transfusion. Because platelets share some of their granule transport systems with other types of hematopoietic cells, they could also be used to screen for other types of immune disorders, including FHL4 and FHL5.

## Acknowledgments

The authors are grateful to all of the participating patients, their families, and the referring physicians for their generous cooperation in this study.

This study was supported by grants from The Morinaga Foundation for Health and Nutrition; from the Japanese Ministry of

Education, Culture, Sports, Science, and Technology; and from the Japanese Ministry of Health, Labor, and Welfare.

## Authorship

Contribution: T.Y., R.N., T.N., H.H., and H.T. designed the research; Y.M., K.I., and M.S. performed the Western blot and flow cytometric analyses; K.O. and O.O. performed the genetic analyses; R.S. and H.H. prepared the anti-Munc13-4 antibodies and started the FHL3 screening; Y.M., T.Y., R.S., K.I., H.S., J.A.,

N.T., T.K., R.N., E.I., T.N., H.H., and T.H. analyzed and discussed the results; and Y.M., T.Y., and T.H. wrote the manuscript.

Conflict-of-interest disclosure: The authors declare no competing financial interests.

Correspondence: Takahiro Yasumi, Department of Pediatrics, Kyoto University Graduate School of Medicine, 54 Kawahara-cho, Shogoin, Sakyo-ku, Kyoto, 606-8507 Japan; e-mail: yasumi@kuhp.kyoto-u.ac.jp or Hisanori Horiuchi, Department of Molecular and Cellular Biology, Institute of Development, Aging and Cancer, Tohoku University, 4-1 Seiryomachi, Aoba-ku, Sendai 980-8575 Japan; e-mail: horiuchi@idac.tohoku.ac.jp.

## References

- Fischer A, Latour S, de Saint Basile G. Genetic defects affecting lymphocyte cytotoxicity. *Curr Opin Immunol*. 2007;19(3):348-353.
- Hong W. Cytotoxic T lymphocyte exocytosis: bring on the SNAREs! *Trends Cell Biol*. 2005;15(12):644-650.
- Ménasché G, Feldmann J, Fischer A, de Saint Basile G. Primary hemophagocytic syndromes point to a direct link between lymphocyte cytotoxicity and homeostasis. *Immunol Rev*. 2005;203:165-179.
- Janka GE. Familial and acquired hemophagocytic lymphohistiocytosis. *Eur J Pediatr*. 2007;166(2):95-109.
- Gupta S, Weitzman S. Primary and secondary hemophagocytic lymphohistiocytosis: clinical features, pathogenesis and therapy. *Expert Rev Clin Immunol*. 2010;6(1):137-154.
- Créput C, Galicier L, Buyse S, Azoulay E. Understanding organ dysfunction in hemophagocytic lymphohistiocytosis. *Intensive Care Med*. 2008;34(7):1177-1187.
- Stapp S, Dufourcq-Lagelouse R, Le Deist F, et al. Perforin gene defects in familial hemophagocytic lymphohistiocytosis. *Science*. 1999;286(5446):1957-1959.
- Feldmann J, Callebaut I, Raposo G, et al. Munc13-4 is essential for cytolytic granules fusion and is mutated in a form of familial hemophagocytic lymphohistiocytosis (FHL3). *Cell*. 2003;115(4):461-473.
- zur Stadt U, Schmidt S, Kasper B, et al. Linkage of familial hemophagocytic lymphohistiocytosis (FHL) type-4 to chromosome 6q24 and identification of mutations in syntaxin 11. *Hum Mol Genet*. 2005;14(6):827-834.
- zur Stadt U, Rohr J, Seifert W, et al. Familial hemophagocytic lymphohistiocytosis type 5 (FHL-5) is caused by mutations in Munc18-2 and impaired binding to syntaxin 11. *Am J Hum Genet*. 2009;85(4):482-492.
- Côte M, Ménager M, Burgess A, et al. Munc18-2 deficiency causes familial hemophagocytic lymphohistiocytosis type 5 and impairs cytotoxic granule exocytosis in patient NK cells. *J Clin Invest*. 2009;119(12):3765-3773.
- Cetica V, Pende D, Griffiths GM, Aricò M. Molecular basis of familial hemophagocytic lymphohistiocytosis. *Haematologica*. 2010;95(4):538-541.
- Perez N, Virelizier JL, Arenzana-Seisdedos F, Fischer A, Griscelli C. Impaired natural killer activity in lymphohistiocytosis syndrome. *J Pediatr*. 1984;104(4):569-573.
- Aricò M, Nespoli L, Maccario R, et al. Natural cytotoxicity impairment in familial hemophagocytic lymphohistiocytosis. *Arch Dis Child*. 1988;63(3):292-296.
- Schneider EM, Lorenz I, Müller-Rosenberger M, Steinbach G, Kron M, Janka-Schaub GE. Hemophagocytic lymphohistiocytosis is associated with deficiencies of cellular cytolysis but normal expression of transcripts relevant to killer-cell-induced apoptosis. *Blood*. 2002;100(8):2891-2898.
- Ishii E, Ueda I, Shirakawa R, et al. Genetic subtypes of familial hemophagocytic lymphohistiocytosis: correlations with clinical features and cytotoxic T lymphocyte/natural killer cell functions. *Blood*. 2005;105(9):3442-3448.
- Schneider EM, Lorenz I, Walthert P, Janka-Schaub GE. Natural killer deficiency: a minor or major factor in the manifestation of hemophagocytic lymphohistiocytosis? *J Pediatr Hematol Oncol*. 2003;25(9):680-683.
- Grom AA, Villanueva J, Lee S, Goldmuntz EA, Passo MH, Filipovich A. Natural killer cell dysfunction in patients with systemic-onset juvenile rheumatoid arthritis and macrophage activation syndrome. *J Pediatr*. 2003;142(3):292-296.
- Grom AA. Natural killer cell dysfunction: A common pathway in systemic-onset juvenile rheumatoid arthritis, macrophage activation syndrome, and hemophagocytic lymphohistiocytosis? *Arthritis Rheum*. 2004;50(3):689-698.
- Horne A, Zheng C, Lorenz I, et al. Subtyping of natural killer cell cytotoxicity deficiencies in hemophagocytic lymphohistiocytosis provides therapeutic guidance. *Br J Haematol*. 2005;129(5):658-666.
- Kogawa K, Lee SM, Villanueva J, Marmer D, Sumegi J, Filipovich AH. Perforin expression in cytotoxic lymphocytes from patients with hemophagocytic lymphohistiocytosis and their family members. *Blood*. 2002;99(1):61-66.
- Alter G, Malenfant JM, Altfeld M. CD107a as a functional marker for the identification of natural killer cell activity. *J Immunol Methods*. 2004;294(1-2):15-22.
- Marcenaro S, Gallo F, Martini S, et al. Analysis of natural killer-cell function in familial hemophagocytic lymphohistiocytosis (FHL): defective CD107a surface expression heralds Munc13-4 defect and discriminates between genetic subtypes of the disease. *Blood*. 2006;108(7):2316-2323.
- Bryceson YT, Rudd E, Zheng C, et al. Defective cytotoxic lymphocyte degranulation in syntaxin-11 deficient familial hemophagocytic lymphohistiocytosis 4 (FHL4) patients. *Blood*. 2007;110(6):1906-1915.
- Shirakawa R, Higashi T, Tabuchi A, et al. Munc13-4 is a GTP-Rab27-binding protein regulating dense core granule secretion in platelets. *J Biol Chem*. 2004;279(11):10730-10737.
- Febbraio M, Silverstein RL. Identification and characterization of LAMP-1 as an activation-dependent platelet surface glycoprotein. *J Biol Chem*. 1990;265(30):18531-18537.
- Ren Q, Wimmer C, Chicka MC, et al. Munc13-4 is a limiting factor in the pathway required for platelet granule release and hemostasis. *Blood*. 2010;116(6):869-877.
- Nagai K, Yamamoto K, Fujiwara H, et al. Subtypes of familial hemophagocytic lymphohistiocytosis in Japan based on genetic and functional analyses of cytotoxic T lymphocytes. *PLoS ONE*. 2010;5(11):e14173.
- Rohr J, Beutel K, Maul-Pavicic A, et al. Atypical familial hemophagocytic lymphohistiocytosis due to mutations in UNC13D and STXB2 overlaps with primary immunodeficiency diseases. *Haematologica*. 2010;95(12):2080-2087.
- Stinchcombe J, Bossi G, Griffiths G. Linking albinism and immunity: the secrets of secretory lysosomes. *Science*. 2004;305(5680):55-59.
- Ren Q, Ye S, Whiteheart SW. The platelet release reaction: just when you thought platelet secretion was simple. *Curr Opin Hematol*. 2008;15(5):537-541.

# Gain-of-function human *STAT1* mutations impair IL-17 immunity and underlie chronic mucocutaneous candidiasis

Luyan Liu,<sup>1</sup> Satoshi Okada,<sup>2</sup> Xiao-Fei Kong,<sup>2</sup> Alexandra Y. Kreins,<sup>2</sup> Sophie Cypowj,<sup>2</sup> Avinash Abhyankar,<sup>2</sup> Julie Toubiana,<sup>3</sup> Yuval Itan,<sup>2</sup> Magali Audry,<sup>2</sup> Patrick Nitschke,<sup>4</sup> Cécile Masson,<sup>4</sup> Beata Toth,<sup>9</sup> Jérôme Flatot,<sup>1</sup> Mélanie Migaud,<sup>1</sup> Maya Chrabieh,<sup>1</sup> Tatiana Kochetkov,<sup>2</sup> Alexandre Bolze,<sup>1,2</sup> Alessandro Borghesi,<sup>1</sup> Antoine Toulon,<sup>5</sup> Julia Hiller,<sup>10</sup> Stefanie Eyerich,<sup>10</sup> Kilian Eyerich,<sup>10,11</sup> Vera Gulácsy,<sup>9</sup> Ludmyla Chernyshova,<sup>12</sup> Viktor Chernyshov,<sup>13</sup> Anastasia Bondarenko,<sup>12</sup> Rosa María Cortés Grimaldo,<sup>14</sup> Lizbeth Blancas-Galicia,<sup>15</sup> Ileana Maria Madrigal Beas,<sup>14</sup> Joachim Roesler,<sup>16</sup> Klaus Magdorf,<sup>17</sup> Dan Engelhard,<sup>18</sup> Caroline Thumerelle,<sup>19</sup> Pierre-Régis Burgel,<sup>20</sup> Miriam Hoernes,<sup>21</sup> Barbara Drexel,<sup>21</sup> Reinhard Seger,<sup>21</sup> Theresia Kusuma,<sup>22</sup> Annette F. Jansson,<sup>22</sup> Julie Sawalle-Belohradsky,<sup>22</sup> Bernd Belohradsky,<sup>22</sup> Emmanuelle Jouanguy,<sup>1,2</sup> Jacinta Bustamante,<sup>1</sup> Mélanie Bué,<sup>23</sup> Nathan Karin,<sup>24</sup> Gizi Wildbaum,<sup>24</sup> Christine Bodemer,<sup>5</sup> Olivier Lortholary,<sup>6</sup> Alain Fischer,<sup>7</sup> Stéphane Blanche,<sup>7</sup> Saleh Al-Muhsen,<sup>24</sup> Janine Reichenbach,<sup>21</sup> Masao Kobayashi,<sup>26</sup> Francisco Espinosa Rosales,<sup>15</sup> Carlos Torres Lozano,<sup>14</sup> Sara Sebnem Kilic,<sup>27</sup> Matias Oleastro,<sup>28</sup> Amos Etzioni,<sup>24</sup> Claudia Traidl-Hoffmann,<sup>10,11</sup> Ellen D. Renner,<sup>22</sup> Laurent Abel,<sup>1,2</sup> Capucine Picard,<sup>1,6,8</sup> László Maródi,<sup>9</sup> Stéphanie Boisson-Dupuis,<sup>1,2</sup> Anne Puel,<sup>1</sup> and Jean-Laurent Casanova<sup>1,2,7,25</sup>

<sup>1</sup>Laboratory of Human Genetics of Infectious Diseases, Necker Branch, Necker Medical School, Institut National de la Santé et de la Recherche Médicale U980 and University Paris Descartes, 75015 Paris, France

<sup>2</sup>St. Giles Laboratory of Human Genetics of Infectious Diseases, Rockefeller Branch, The Rockefeller University, New York, NY 10065

<sup>3</sup>Department of Pediatrics, <sup>4</sup>Bioinformatics Unit, <sup>5</sup>Department of Dermatology, <sup>6</sup>Department of Infectious Diseases, <sup>7</sup>Pediatric Hematology-Immunology Unit, and <sup>8</sup>Center for Immunodeficiency, Necker Hospital, AP-HP, and University Paris Descartes, 75015 Paris, France

<sup>9</sup>Department of Infectious and Pediatric Immunology, Medical and Health Science Center, University of Debrecen, 4032 Debrecen, Hungary

<sup>10</sup>Center for Allergy and Environment, Helmholtz Center/TUM, 80802 Munich, Germany

<sup>11</sup>Department of Dermatology, Technische Universität, 80802 Munich, Germany

<sup>12</sup>Department of Pediatric Infectious Diseases and Clinical Immunology, National Medical Academy for Post-Graduate Education, 01024 Kiev, Ukraine

<sup>13</sup>Laboratory of Immunology, Institute of Pediatrics, Obstetrics, and Gynecology, National Academy of Medical Sciences, 01024 Kiev, Ukraine

<sup>14</sup>Allergy and Immunology Department, UMAE-HE-CMNO-IMMS, 44500 Guadalajara, Mexico

<sup>15</sup>National Institute of Pediatrics, 04530 Mexico City, Mexico

<sup>16</sup>Department of Pediatrics, University Hospital Carl Gustav Carus, 01307 Dresden, Germany

<sup>17</sup>Department of Pediatric Pneumology and Immunology, Charité Medical School of Berlin, 11117 Berlin, Germany

<sup>18</sup>Department of Pediatrics, Hadassah University Hospital, 91120 Jerusalem, Israel

<sup>19</sup>Pneumology and Allergology Unit, Hospital Jeanne de Flandres, 59037 Lille, France

<sup>20</sup>Pneumology and UPRES EA 2511, Hospital Cochin, AP-HP, 75014 Paris, France

<sup>21</sup>Division of Immunology, Hematology, and BMT, Children's Research Center, Children's Hospital, University of Zurich, 8032 Zurich, Switzerland

<sup>22</sup>University Children's Hospital at Dr. von Haunersches Kinderspital, Ludwig Maximilian University, 80337 Munich, Germany

<sup>23</sup>University Hospital Center of Brest, 29609 Brest, France

<sup>24</sup>Rappaport Faculty of Medicine, Technion, 31096 Haifa, Israel.

<sup>25</sup>Prince Naif Center for Immunology Research, Department of Pediatrics, College of Medicine, King Saud University, Riyadh, 11461 Saudi Arabia

<sup>26</sup>Department of Pediatrics, Hiroshima University Graduate School of Biomedical Sciences, 739-8511 Hiroshima, Japan

<sup>27</sup>Department of Pediatrics, Uludag University School of Medicine, 16059 Bursa, Turkey

<sup>28</sup>National Children's Hospital Prof. Dr. Juan P. Garrahan, 12049 Buenos Aires, Argentina

L. Liu, S. Okada, X.-F. Kong, A.Y. Kreins, and S. Cypowj contributed equally to this paper.

A. Abhyankar, J. Toubiana, Y. Itan, M. Audry, P. Nitschke, C. Masson, and B. Toth contributed equally to this paper.

S. Al-Muhsen, J. Reichenbach, M. Kobayashi, F. Espinoza Rosales, C. Torres Lozano, S. Sebnem Kilic, M. Oleastro, A. Etzioni, C. Traidl-Hoffmann, E.D. Renner, L. Abel, and C. Picard contributed equally to this paper.

L. Maródi, S. Boisson-Dupuis, A. Puel, and J.-L. Casanova contributed equally to this paper.

© 2011 Liu et al. This article is distributed under the terms of an Attribution-Noncommercial-Share Alike-No Mirror Sites license for the first six months after the publication date (see <http://www.rupress.org/terms>). After six months it is available under a Creative Commons License (Attribution-Noncommercial-Share Alike 3.0 Unported license, as described at <http://creativecommons.org/licenses/by-nc-sa/3.0/>).

## CORRESPONDENCE

Anne Puel:  
anne.puel@inserm.fr  
OR

Jean-Laurent Casanova:  
jean-laurent.casanova@rockefeller.edu

Abbreviations used: AD, autosomal dominant; AR, autosomal recessive; CMC, chronic mucocutaneous candidiasis; CMCD, CMC disease; EMSA, electrophoretic mobility shift assay; GAS,  $\gamma$ -activated sequence; ISRE, IFN-stimulated response element; MSMD, Mendelian susceptibility to mycobacterial disease; WB, Western blotting.

The Rockefeller University Press \$30.00  
J. Exp. Med. Vol. 208 No. 8 1635-1648  
[www.jem.org/cgi/doi/10.1084/jem.20110958](http://www.jem.org/cgi/doi/10.1084/jem.20110958)

Chronic mucocutaneous candidiasis disease (CMCD) may be caused by autosomal dominant (AD) IL-17F deficiency or autosomal recessive (AR) IL-17RA deficiency. Here, using whole-exome sequencing, we identified heterozygous germline mutations in *STAT1* in 47 patients from 20 kindreds with AD CMCD. Previously described heterozygous *STAT1* mutant alleles are loss-of-function and cause AD predisposition to mycobacterial disease caused by impaired STAT1-dependent cellular responses to IFN- $\gamma$ . Other loss-of-function *STAT1* alleles cause AR predisposition to intracellular bacterial and viral diseases, caused by impaired STAT1-dependent responses to IFN- $\alpha/\beta$ , IFN- $\gamma$ , IFN- $\lambda$ , and IL-27. In contrast, the 12 AD CMCD-inducing *STAT1* mutant alleles described here are gain-of-function and increase STAT1-dependent cellular responses to these cytokines, and to cytokines that predominantly activate STAT3, such as IL-6 and IL-21. All of these mutations affect the coiled-coil domain and impair the nuclear dephosphorylation of activated STAT1, accounting for their gain-of-function and dominance. Stronger cellular responses to the STAT1-dependent IL-17 inhibitors IFN- $\alpha/\beta$ , IFN- $\gamma$ , and IL-27, and stronger STAT1 activation in response to the STAT3-dependent IL-17 inducers IL-6 and IL-21, hinder the development of T cells producing IL-17A, IL-17F, and IL-22. Gain-of-function *STAT1* alleles therefore cause AD CMCD by impairing IL-17 immunity.

Chronic mucocutaneous candidiasis (CMC) is characterized by persistent or recurrent disease of the nails, skin, oral, or genital mucosae caused by *Candida albicans* (Puel et al., 2010b). CMC may be caused by various inborn errors of immunity. CMC is one of a multitude of infectious diseases observed in patients with broad and profound T cell deficiencies. In contrast, patients with the autosomal dominant (AD) hyper IgE syndrome, caused by dominant-negative mutations of *STAT3*, are susceptible principally to CMC and staphylococcal diseases of the lungs and skin (Minegishi, 2009). These patients have very low proportions of circulating IL-17A- and IL-22-producing T cells, probably because of impaired responses to IL-6, IL-21, and/or IL-23 (de Beaucoudrey et al., 2008; Ma et al., 2008; Milner et al., 2008; Renner et al., 2008; Minegishi et al., 2009). Patients with autosomal recessive (AR) IL-12p40 or IL-12R $\beta$ 1 deficiency suffer from Mendelian susceptibility to mycobacterial disease (MSMD) and occasionally develop mild CMC (Filipe-Santos et al., 2006; de Beaucoudrey et al., 2010). Some have low proportions of IL-17A- and IL-22-producing T cells, presumably because of the abolition of IL-23 responses (de Beaucoudrey et al., 2008, 2010). The proportion of IL-17A-producing T cells was also found to be low in a family with AR *CARD9* deficiency, dermatophytosis, invasive candidiasis, and CMC (Glocker et al., 2009). Finally, CMC is the only infection in patients with autoimmune polyendocrinopathy syndrome type 1, who have high titers of neutralizing autoantibodies against IL-17A, IL-17F, and IL-22 (Kisand et al., 2010; Puel et al., 2010a). Thus, regardless of the underlying illness, CMC pathogenesis apparently involves the impairment of IL-17A, IL-17F, and IL-22 immunity (Puel et al., 2010b).

The pathogenesis of CMC was eventually deciphered through investigations of patients with CMC disease (CMCD), in which CMC is isolated, with no other infectious or autoimmune signs (Kirkpatrick, 2001; Puel et al., 2010b). The definition of CMCD is not absolute, as illustrated in some patients by cutaneous staphylococcal disease, which is milder than that in patients with AD hyper IgE syndrome (Herrod, 1990), or by autoimmune features affecting the thyroid in particular, although fewer such features are observed than in patients with autoimmune polyendocrinopathy syndrome

type 1 (Atkinson et al., 2001). It is unclear whether CMCD, with these or other manifestations (Shama and Kirkpatrick, 1980; Bentur et al., 1991; Germain et al., 1994), is immunologically and genetically related to pure CMCD. Low proportions of IL-17A-producing T cells have been documented in five patients with CMCD (Eyerich et al., 2008). Moreover, a candidate gene approach centered on IL-17 immunity recently revealed the first genetic etiologies of pure CMCD. In a consanguineous family from Morocco, a child with CMCD was found to display AR complete IL-17RA deficiency (Puel et al., 2011). His leukocytes and fibroblasts did not respond to IL-17A or IL-17F homodimers, or to IL-17A/F heterodimers. Four patients from an Argentinean family were shown to harbor dominant-negative mutations in the *IL17F* gene (Puel et al., 2011). Mutated IL-17F-containing homodimers and heterodimers were produced in normal amounts but were not biologically active, as they were unable to bind to the IL-17 receptor. Morbid mutations in *IL17RA* and *IL17F* demonstrated that CMCD could be caused by inborn errors of IL-17 immunity. However, no genetic etiology has yet been identified for most patients with CMCD. We set out to identify new genetic etiologies of CMCD through a recently developed genome-wide approach based on whole-exome sequencing (Alcais et al., 2010; Bolze et al., 2010; Byun et al., 2010; Ng et al., 2010).

## RESULTS

We investigated one sporadic case and the probands from five multiplex kindreds with AD CMCD, by whole-exome sequencing. The annotated data were analyzed with sequence analysis software that had been developed in-house and made it possible to analyze and compare several exome sequences simultaneously. A hierarchy of candidate variations was generated by filtering out known polymorphisms reported in dbSNP and 1,000-genome databases. We also used our own database of 250 exomes to filter out unreported polymorphisms (Table S1). The only relevant gene displaying heterozygous variations in at least four of the six unrelated patients with AD CMCD was *STAT1* (Fig. 1, A and B, Kindreds A, B, G, and L; Table I; and Table S2). Three different *STAT1* mutations were found in four patients; they were confirmed by Sanger

sequencing and shown to be missense mutations. All these mutations affected the coiled-coil domain, which plays a key role in unphosphorylated STAT1 dimerization and STAT1 nuclear dephosphorylation (Fig. 1, A and C; Chen et al., 1998; Levy and Darnell, 2002; Braunstein et al., 2003; Zhong et al., 2005; Hoshino et al., 2006; Mertens et al., 2006). We therefore sequenced the corresponding coding region of *STAT1* (exons 6 to 10) in another 106 patients, including 57 with sporadic CMCD and 49 from 22 multiplex kindreds with AD CMCD. 29 patients from 16 kindreds were heterozygous for a *STAT1* missense mutation (Fig. 1, A and B, Kindreds C-F, H-K, and M-T; Fig. 1 C; and Table I; Table S3). In total, 36 patients from 20 kindreds were heterozygous for 1 of the 12 missense mutations identified that affected the coiled-coil domain of STAT1. 11 other CMCD patients in these kindreds were not genotyped. The intrafamilial segregation of the mutations was consistent with an AD trait, as all patients with CMCD from the kindreds tested were heterozygous, whereas none of these mutations was found in the heterozygous state in any of the healthy relatives tested (Fig. 1 B). Moreover, the *STAT1* haplotypes for common SNPs indicated that the five recurrent mutations were caused by mutation hotspots rather than founder effects (unpublished data). Finally, the mutations were found to have occurred de novo in at least four kindreds, which is consistent with a high clinical penetrance of these alleles. The mutations were not found in the National Center for Biotechnology Information, Ensembl, and dbSNP databases. They were also absent from 1,052 controls from 52 ethnic groups in the Centre d'Etude du Polymorphisme Humain and Human Genome Diversity panels, suggesting that they were rare, CMCD-inducing variants rather than irrelevant polymorphisms.

The 12 missense mutations were not conservative and were therefore predicted to affect protein structure and function. Moreover, most of the affected residues were found to have been conserved throughout evolution in the species in which *STAT1* had been sequenced (Table S3). Accordingly, POLYphen II predicted that all but one of these mutations would be possibly or probably damaging (Adzhubei et al., 2010; Table S3). None of the previously described nine patients with AD STAT1 deficiency and MSMD was heterozygous for mutations affecting the coiled-coil domain (Fig. 1, A and C; Dupuis et al., 2001; Chapgier et al., 2006a; Averbuch et al., 2011; unpublished data). However, three of the eight patients with AR STAT1 deficiency and susceptibility to intracellular bacterial and viral diseases, who, like their heterozygous relatives, did not display CMC, carried mutations affecting the coiled-coil domain (Fig. 1, A and C; Chapgier et al., 2009; Chapgier et al., 2006b; Dupuis et al., 2003; Kong et al., 2010; Kristensen et al., 2011; Averbuch et al., 2011). These three patients from two kindreds carried the K201N or K211R mutation (Kong et al., 2010; Kristensen et al., 2011). Nevertheless, the three-dimensional structure of phosphorylated STAT1 molecules revealed that the 12 CMCD-linked missense mutations affected a cluster of residues located in a specific pocket of the coiled-coil domain, near residues essential for STAT1

dephosphorylation (Fig. 1 C; Chen et al., 1998; Zhong et al., 2005; Mertens et al., 2006). In contrast, the other two morbid mutations (K201N and K211R) affect residues located on the other side of the coiled-coil domain (Fig. 1 C). Moreover, these two hypomorphic alleles were shown to be pathogenic not because they were missense, but because they promoted the splicing out of exon 8, resulting in AR partial STAT1 deficiency, with the production of small amounts of intrinsically functional STAT1 molecules (Kong et al., 2010; Kristensen et al., 2011). These genetic data strongly suggest that heterozygous missense mutations in the coiled-coil domain of STAT1 may cause AD CMCD in a large fraction of patients. Nevertheless, the occurrence of other germline mutations in *STAT1* in patients without CMC and with an AD or AR predisposition to other infectious diseases raised questions about whether these mutations were really responsible for CMCD and the underlying mechanism of disease.

We functionally characterized the CMCD-causing *STAT1* allele R274Q, which was found in four kindreds (Fig. 1 B and Table I). We compared it with a WT and an MSMD-causing loss-of-function *STAT1* allele (L706S; Dupuis et al., 2001). We transfected STAT1-deficient U3C fibrosarcoma cells with WT, R274Q, or L706S *STAT1* alleles. Upon stimulation with IFN- $\alpha$ , IFN- $\gamma$ , or IL-27, cells transfected with the R274Q allele responded two to three times more strongly than those transfected with the WT allele, as shown by measurement of the induction of  $\gamma$ -activated sequence (GAS)-dependent reporter gene transcription activity, with mock- and L706S-transfected cells serving as negative controls (Fig. 2 A and Fig. S1 A). All *STAT1* alleles were expressed at an equal strength, as shown by Western blotting (WB; Fig. 2 B). Higher levels of STAT1 phosphorylation were observed for the R274Q allele than for the WT allele after stimulation with IFN- $\gamma$ , IFN- $\alpha$ , and IL-27, whereas STAT3 phosphorylation levels were similar for the two alleles (Fig. 2 B). In contrast, the induction of IFN-stimulated response element (ISRE)-dependent transcription activity by IFN- $\alpha$  was normal (Fig. S1, B and C). In the same experimental conditions, the other 10 CMCD-associated *STAT1* alleles tested were also gain-of-function, unlike the K201N and K211R alleles (Fig. S1 D). Upon stimulation with IFN- $\gamma$ , IFN- $\alpha$ , or IL-27, an increase in GAS-binding activity was detected in cells transfected with the R274Q allele (Fig. S1 E). Accordingly, the transcription of the *CXCL9* and *CXCL10* target genes was enhanced (Fig. 2, C and D). Overall, these data indicate that at least 11 of the 12 CMCD-linked *STAT1* missense alleles are intrinsically gain-of-function.

The mechanism involved an increase in STAT1 tyrosine 701 residue phosphorylation, as shown for R274Q by WB after stimulation with IFN- $\alpha$ , IFN- $\gamma$ , and IL-27 (Fig. 2 B). STAT1 was not constitutively activated, and STAT3 was normally activated in R274Q-transfected cells (Fig. 2 B and not depicted). Almost all the mutant STAT1 molecules, which were phosphorylated in response to IFN- $\gamma$ , translocated to and accumulated in the nucleus, as shown by immunofluorescence (Fig. S1 F). WB showed R274Q STAT1 to be more

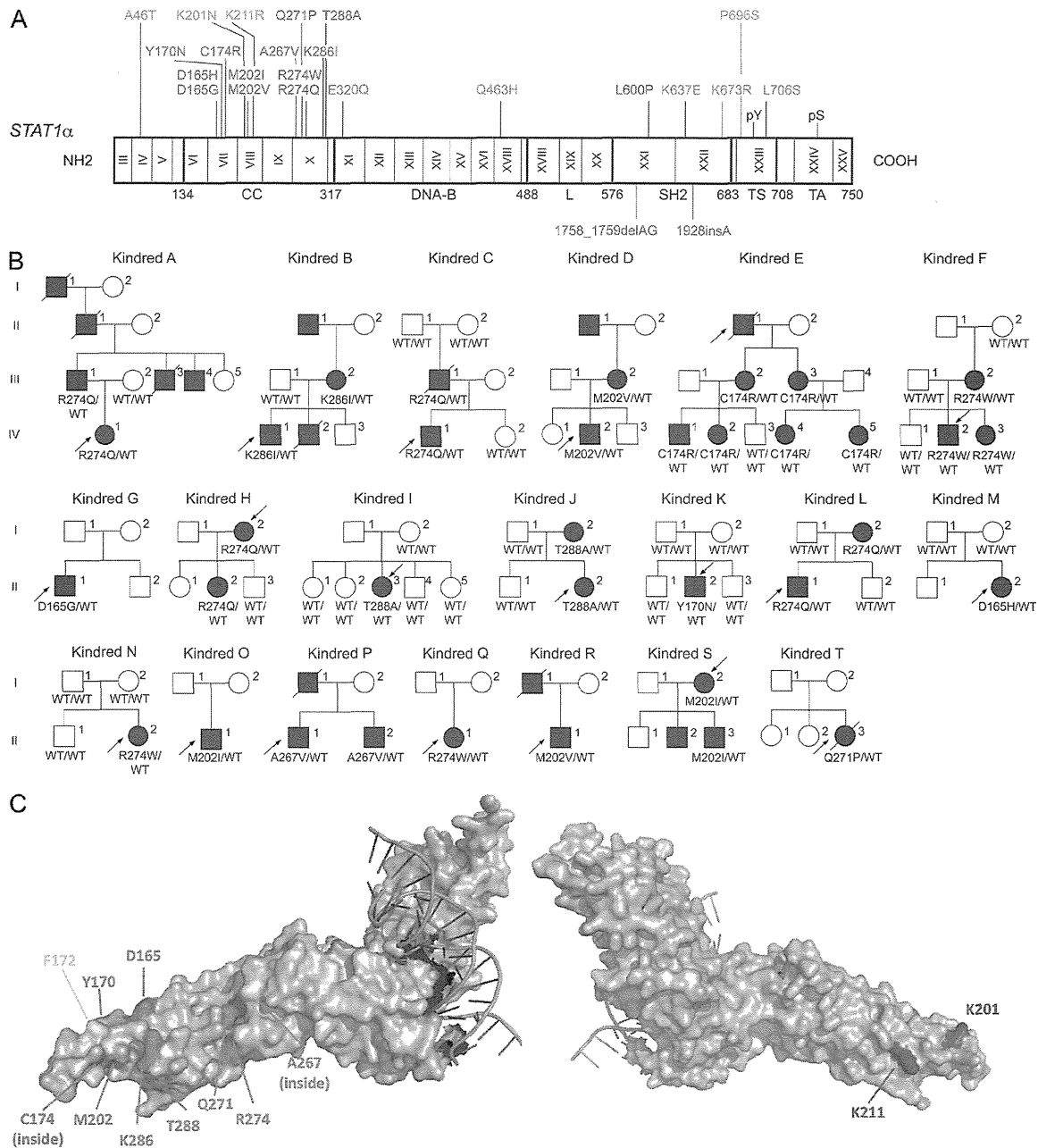


**Figure 1. Heterozygous missense mutations affecting the STAT1 coiled-coil domain in kindreds with AD CMCD.** (A) The human *STAT1*  $\alpha$  isoform is shown, with its known pathogenic mutations. Coding exons are numbered with roman numerals and delimited by a vertical bar. Regions corresponding to the coiled-coil domain (CC), DNA-binding domain (DNA-B), linker domain (L), SH2 domain (SH2), tail segment domain (TS), and transactivator domain (TA) are indicated, together with their amino-acid boundaries, and are delimited by bold lines. Tyr701 (pY) and Ser727 (pS) are indicated. Mutations in green are dominant and associated with partial STAT1 deficiency and MSMD. Mutations in brown are recessive and associated with complete STAT1 deficiency and intracellular bacterial and viral disease. Mutations in blue are recessive and associated with partial STAT1 deficiency and intracellular bacterial and/or viral disease. Mutations in red are dominant and associated with a gain-of-function of STAT1 and CMCD. (B) Pedigrees of 20 families with AD “gain-of-function” *STAT1* mutations. Each kindred is designated by a letter (A to T), each generation is designated by a roman numeral (I–II–III–IV), and each individual is designated by an Arabic numeral (each individual studied is identified by a code of this type, organized from left to right). Black indicates CMCD patients. The probands are indicated by arrows. When tested, the genotype for *STAT1* is indicated below each individual. (C) Three-dimensional structure of phosphorylated STAT1 in complex with DNA. Connolly surface representation, with the following amino acids highlighted: red, amino acids mutated in patients with CMCD; blue, amino acids located in the coiled-coil domain and mutated in patients with MSMD and viral diseases; yellow, amino acids identified in vitro as affecting the dephosphorylation process.

**Table I.** Summary of the clinical and genetic data for the patients

Patient	Age at presentation	Origin	Clinical features of CMC	Cause of death (age/yr)	Autoimmunity	Genotype
A-I-1	-	France	Nails	Not related to the disease (old age)	None	-
A-II-1	-	France	Nails	Not related to the disease (old age)	None	-
A-III-1	1 mo	France	Nails, oral cavity, oropharynx, genital mucosa		None	WT/R274Q
A-III-3	-	France	Nails, oral cavity	Not related to the disease (40)	None	-
A-III-4	-	France	Nails, oral cavity		None	-
A-IV-1	1 mo	France	Nails, oral cavity, oropharynx		None	WT/R274Q
B-II-1	-	France	-		None	-
B-III-2	3 yr	France	Skin, nails, oral cavity, oropharynx, genital mucosa		None	WT/K286I
B-IV-1	5 yr	France & Congo	Skin, nails, oral cavity, oropharynx		None	WT/K286I
B-IV-2	5 mo	France & Congo	Skin, nails, oral cavity, oropharynx	Cerebral aneurysm (8)	None	-
C-III-1	-	Turkey	Nails, oral cavity, genital mucosa	Cerebral aneurysm (34)	Thyroid autoimmunity	WT/R274Q
C-IV-1	-	Turkey	Nails, oral cavity		None	WT/R274Q
D-II-1	-	France	Nails, oral cavity, genital mucosa		-	-
D-III-2	7 yr	France	Skin, oral cavity, oropharynx		None	WT/M202V
D-IV-2	1 mo	France	Skin, nails, oropharynx		Thyroid autoimmunity	WT/M202V
E-II-1	1 yr	Germany	Skin, oral cavity, oropharynx	Squamous cell carcinoma (54)	-	-
E-III-2	1 yr	Germany	Nails, oral cavity, oropharynx, genital mucosa		Thyroid autoimmunity	WT/C174R
E-III-3	9 mo	Germany	Skin, nails, oral cavity, oropharynx, genital mucosa		Thyroid autoimmunity	WT/C174R
E-IV-1	18 mo	Germany	Skin, oral cavity, oropharynx, genital mucosa		None	WT/C174R
E-IV-2	2 yr	Germany	Skin, oral cavity, oropharynx		Thyroid autoimmunity	WT/C174R
E-IV-4	2 yr	Germany	Skin, oral cavity, oropharynx, genital mucosa		None	WT/C174R
E-IV-5	1 yr	Germany	Skin, nails, oral cavity, oropharynx		None	WT/C174R
F-III-2	1 mo	Argentina	Nails, oral cavity, oropharynx, genital mucosa		-	WT/R274W
F-IV-2	1 mo	Argentina	Skin, nails, oral cavity, oropharynx		-	WT/R274W
F-IV-3	6 mo	Argentina	Nails, oral cavity, genital mucosa		-	WT/R274W
G-II-1	3 mo	Ukrainian	Nails, skin, oral cavity, oropharynx, esophagus		None	WT/D165G
H-I-2	1 yr	Japan	Skin, oropharynx, esophagus		-	WT/R274Q
H-II-2	5 yr	Japan	Oral cavity, oropharynx		-	WT/R274Q
I-II-3	9 mo	Mexico	Skin, nails, oral cavity, genital mucosa		None	WT/T288A
J-I-2	-	Switzerland	Oral cavity, oropharynx		None	WT/T288A
J-II-2	3 mo	Switzerland	Oral cavity, oropharynx		-	WT/T288A
K-II-2	11 mo	Switzerland	Nails, oral cavity, oropharynx		Thyroid autoimmunity	WT/Y170N
L-I-2	7 yr	France	Skin, nails, oropharynx, esophagus		Thyroid autoimmunity	WT/R274Q
L-II-1	1 mo	France	Skin, nails, oropharynx, esophagus		None	WT/R274Q
M-II-2	6 mo	Germany	Skin, nails, oropharynx, genital mucosa		Thyroid autoimmunity	WT/D165H

**Table I.** Summary of the clinical and genetic data for the patients (*Continued*)

Patient	Age at presentation	Origin	Clinical features of CMC	Cause of death (age/yr)	Autoimmunity	Genotype
N-II-2	1 yr	Germany	Skin, nails, oropharynx	Squamous cell carcinoma (54)	None	WT/R274W
O-II-1	18 mo	Germany	Oral cavity, oropharynx		None	WT/M202I
P-I-1	1 yr	Israel	Oropharynx, genital mucosa	Not related to the disease (46)	None	-
P-II-1	<2 yr	Israel	Skin, nails, oropharynx		None	WT/A267V
P-II-2	<2 yr	Israel	Skin, nails, oropharynx		None	WT/A267V
Q-II-1	1 mo	France	Skin, oral cavity, oropharynx, genital mucosa		None	WT/R274W
R-I-1	4 yr	France	Skin, nails, oropharynx	Squamous cell carcinoma (55)	None	-
R-II-1	18 mo	France	Lips, oropharynx		None	WT/M202V
S-I-2	6 mo	France	Skin, oral cavity, oropharynx		Systemic lupus erythematosus	WT/M202I
S-II-2	1 yr	France	Nails		None	-
S-II-3	1 mo	France	Skin, oropharynx		None	WT/M202I
T-II-3	1 yr	Germany	Skin, nails, oropharynx	Squamous cell carcinoma (41)	None	WT/Q271P

None of the patients displays autoantibodies against IL-17A, IL-17F, and IL-22. -, unknown.

strongly phosphorylated than the WT protein in both cytoplasmic and nuclear extracts (Fig. S1 G). The mechanism underlying the gain of R274Q phosphorylation was explored with the tyrosine kinase inhibitor staurosporine and the phosphatase inhibitor pervanadate. The dephosphorylation of IFN- $\gamma$ -activated R274Q STAT1 was impaired by staurosporine, but less than that of the known dephosphorylation mutant F77A (Fig. 2 E; Zhong et al., 2005). In contrast, pervanadate normalized the phosphorylation of R274Q to WT levels (Fig. 2 F). Another CMCD-linked mutation, D165G (Fig. 1, A–C), also resulted in impaired dephosphorylation that could be normalized by adding pervanadate (Fig. 2 F and Fig. S1 H). Thus, at least two CMCD-linked *STAT1* missense alleles (R274Q and D165G) are gain-of-function caused by the impairment of nuclear dephosphorylation. These alleles may therefore enhance cellular responses to cytokines activating STAT1 predominantly and STAT3 to a lesser extent, such as IFN- $\alpha/\beta$ , IFN- $\gamma$ , IFN- $\lambda$ , and IL-27, and possibly also responses to cytokines activating STAT3 predominantly and STAT1 to a lesser extent, such as IL-6, IL-21, IL-22, and IL-23 (Fig. S2).

We investigated the dominance of the *STAT1* alleles at the cellular level by testing EBV-B-transformed (EBV-B) cells and SV-40-transformed dermal fibroblasts from a CMCD patient heterozygous for the *STAT1* R274Q allele. We observed enhanced IFN- $\alpha/\beta$ -, IFN- $\gamma$ -, and IL-27-dependent STAT1 phosphorylation in EBV-B cells from a patient heterozygous for the *STAT1* R274Q allele, as shown by WB (Fig. 3, B and D). Phospho-STAT1 accumulated in the nucleus of R274Q heterozygous SV-40 fibroblasts upon IFN- $\gamma$  stimulation, as well as in EBV-B cells (Fig. 3 I and Fig. S3 D). Moreover, the IFN- $\alpha/\beta$ -, IFN- $\gamma$ -, and IL-27-induced DNA-binding activity of GAF was stronger in cells from the CMCD patient than in those from a healthy control or from a MSMD patient carrying the L706S mutant allele, as shown by electrophoretic mobility

shift assay (EMSA; Fig. 3, A and C). In contrast, the DNA-binding activity of ISGF-3 seemed to be normal in cells from the patient stimulated with IFN- $\alpha/\beta$  (Fig. S3 A). These data strongly suggest that the heterozygous R274Q allele is dominant for STAT1-dependent responses and gain-of-function for GAF-dependent cellular responses to key STAT1-activating cytokines, such as IFN- $\alpha/\beta$ , IFN- $\gamma$ , and IL-27. The mutation may also affect IFN- $\lambda$  responses.

We then tested cytokines that predominantly activate STAT3, rather than STAT1, such as IL-6, IL-21, IL-22, and IL-23 (Hunter, 2005; Kishimoto, 2005; Kastelein et al., 2007; Spolski and Leonard, 2008; Donnelly et al., 2010; Sabat, 2010; Ouyang et al., 2011). Peripheral T cell blasts from a patient displayed normal STAT3 activation in response to IL-23, as shown by WB (Fig. S3 B). No increase in STAT1 phosphorylation was detected in cells from a patient or controls upon IL-23 stimulation. Furthermore, fibroblasts from a patient displayed normal activation of STAT3 in response to IL-22 (Fig. S3 C). In the same conditions, no STAT1 phosphorylation was detected in cells from the patient or controls (unpublished data). In contrast, the levels of STAT1 phosphorylation in response to IL-6 and IL-21 were higher in the patient's EBV-B cells than in cells from healthy controls and from a patient with MSMD heterozygous for the L706S allele, whereas STAT3 activation was normal as shown by WB (Fig. 3, F and H). Consistent with these findings, stronger GAS activity was observed in cells from the patient in response to IL-6 and IL-21 stimulation (Fig. 3, E and G). These data suggest that heterozygous missense mutations in the coiled-coil domain of STAT1 are dominant and gain-of-function for GAF-dependent cellular responses for cytokines that predominantly activate STAT3, such as IL-6 and IL-21. Overall, these data suggest that the *STAT1* alleles are truly responsible for CMCD in these kindreds and raise questions about the immunological basis of CMCD.



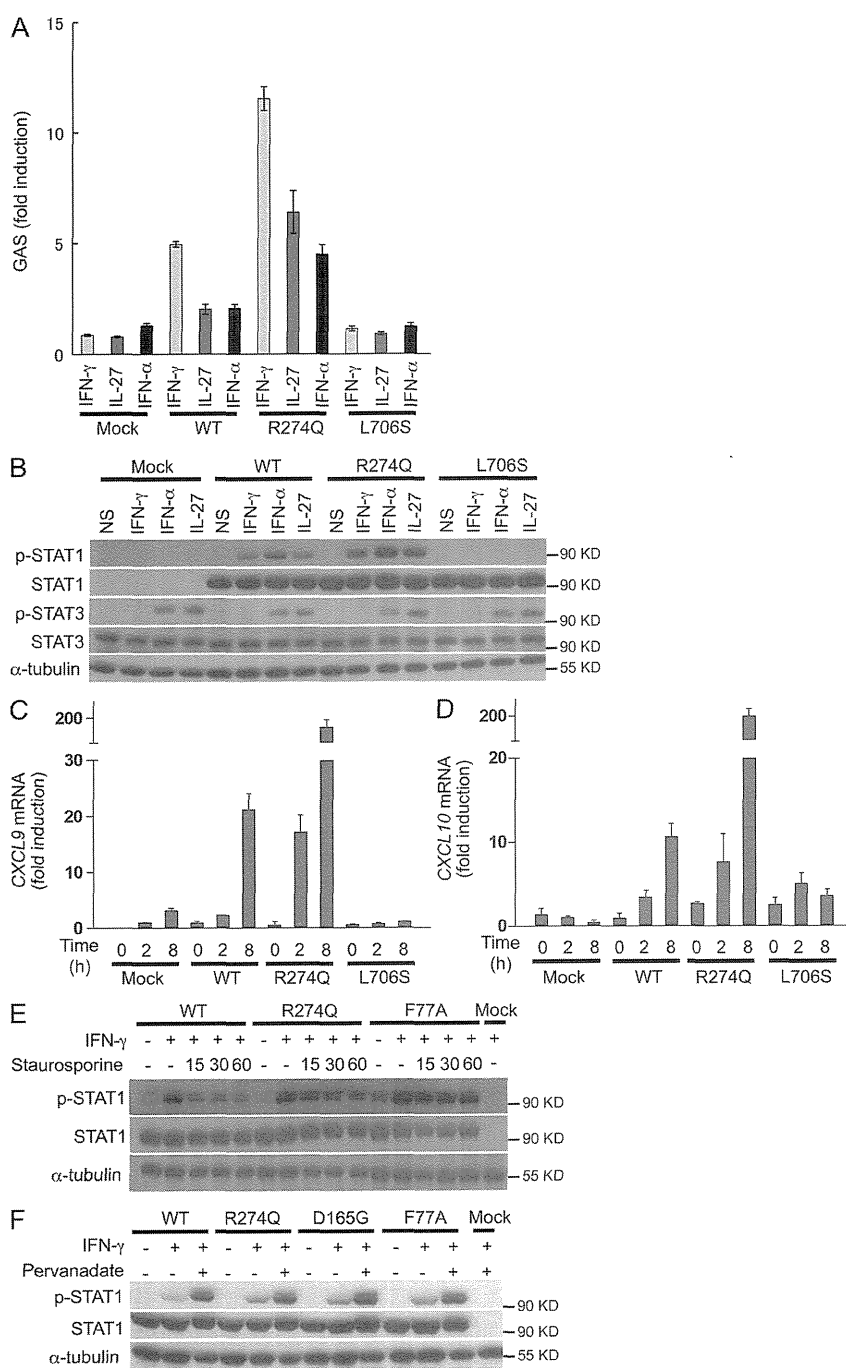


**Figure 2. The mutant R274Q *STAT1* allele is gain-of-phosphorylation and gain-of-function for GAF-dependent cellular responses.** U3C cells were transfected with a mock vector, a WT, or two mutant alleles of *STAT1* (R274Q and L706S). The response to IFN- $\gamma$ , IL-27, and IFN- $\alpha$  was then evaluated by determining luciferase activity of a reporter gene under the control of the GAS promoter (A), and by determining STAT1 and STAT3 phosphorylation by Western blot (B). Experiments were performed at least three times independently. (C and D) Quantitative RT-PCR was used to measure the induction of *CXCL9* (C) and *CXCL10* (D) 2–8 h after stimulation with IFN- $\gamma$ . Experiments were performed two times independently. (E) The nuclear dephosphorylation of STAT1 was tested by WB in U3C cells transfected with a mock vector, WT *STAT1*, the R274Q, or the F77A (a known loss-of-dephosphorylation mutant) *STAT1* mutant alleles, and treated with IFN- $\gamma$  with or without the tyrosine kinase inhibitor staurosporine for the indicated periods of time (in minutes). Three independent experiments were performed. (F) Western blot of U3C cells transfected with mock, WT, R274Q, D165G, and F77A alleles of *STAT1*, nontreated or treated with IFN- $\gamma$  in the absence or presence of the phosphatase inhibitor pervanadate. Two independent experiments were performed. Error bars represent SD of one experiment done in triplicate (Fig. S1 D).

Villarino et al., 2010). Moreover, mouse IFN- $\gamma$  (Feng et al., 2008; Tanaka et al., 2008; Villarino et al., 2010) and human IFN- $\alpha/\beta$  (Chen et al., 2009; Ramgolam et al., 2009) have been shown to antagonize the development of IL-17-producing T cells via STAT1. In addition, IL-6, IL-21, and IL-23 are prominent inducers of IL-17-producing T cells, via a mechanism dependent on STAT3 and antagonized by STAT1 (Hirahara et al., 2010). Finally, we recently showed that in-born errors of IL-17F or IL-17RA were genetic etiologies of CMCD (Puel et al., 2010b, 2011). We thus determined the proportion of IL-17A- and IL-22-producing T cells by flow

cytometry in patients with heterozygous *STAT1* mutations and AD CMCD. The 18 CMCD patients carrying gain-of-function mutations in *STAT1* that were tested had lower proportions of circulating IL-17A- and IL-22-producing T cells ex vivo than 28 healthy controls ( $P < 10^{-4}$ ) and six patients bearing loss-of-function *STAT1* alleles ( $P < 2.10^{-3}$ ; Fig. 4, A and B; and Fig. S4 G). In contrast, they displayed normal proportions of IFN- $\gamma$ -producing T cells (Fig. S4 F).

cytometry in patients with heterozygous *STAT1* mutations and AD CMCD. The 18 CMCD patients carrying gain-of-function mutations in *STAT1* that were tested had lower proportions of circulating IL-17A- and IL-22-producing T cells ex vivo than 28 healthy controls ( $P < 10^{-4}$ ) and six patients bearing loss-of-function *STAT1* alleles ( $P < 2.10^{-3}$ ; Fig. 4, A and B; and Fig. S4 G). In contrast, they displayed normal proportions of IFN- $\gamma$ -producing T cells (Fig. S4 F).

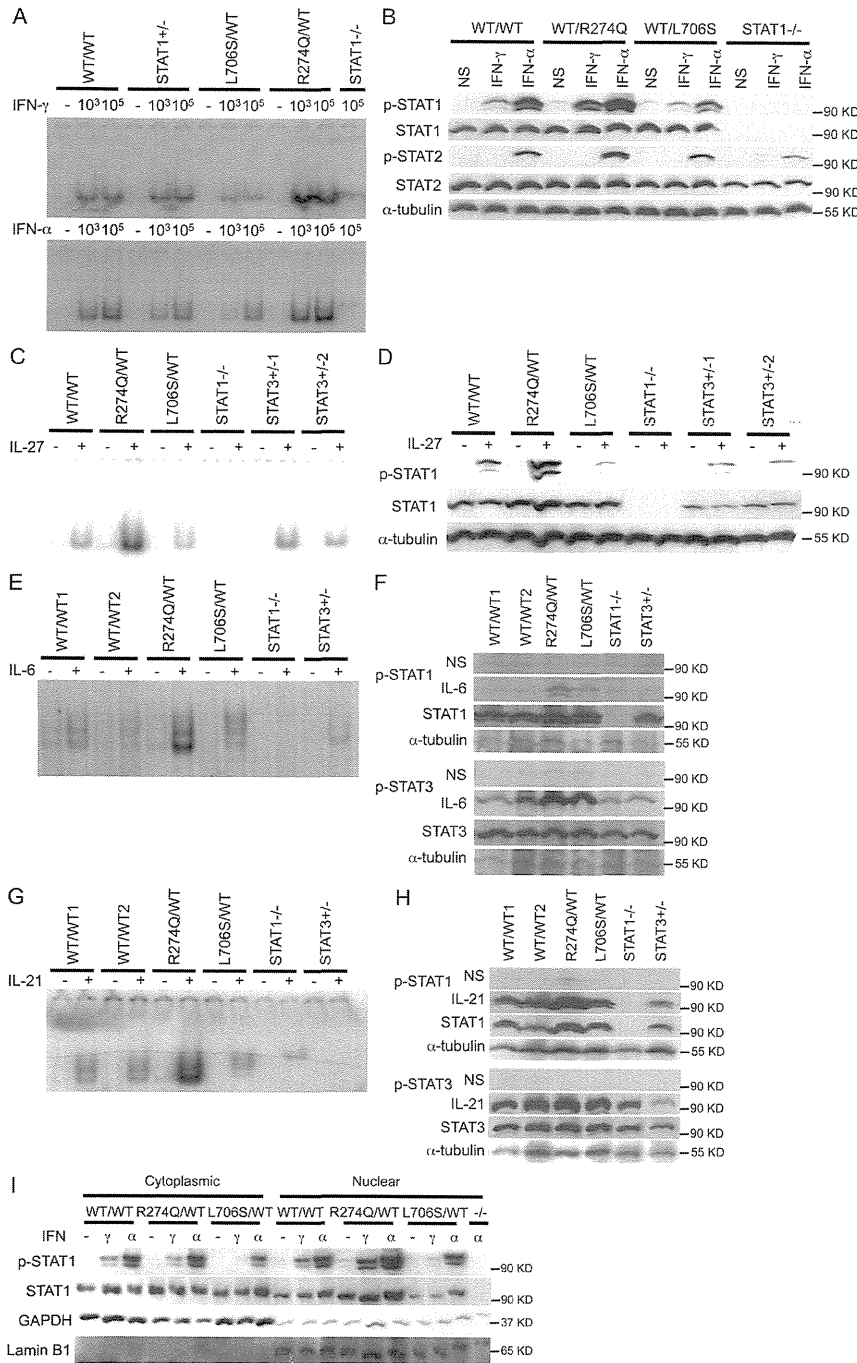


**Figure 3. The mutant R274Q STAT1 allele is dominant for GAF-dependent cellular responses at the cellular level.** The responses of the patient's EBV-B cells (R274Q/WT) were evaluated independently at least twice, by EMSA, with a GAS probe (A, C, E, and G), and by Western blot (B, D, F, and H). This response was compared with that of one or two healthy controls (WT/WT1 and WT/WT2), heterozygous cells with a WT and a loss-of-function STAT1 allele (STAT1<sup>+/-</sup>), cells heterozygous for a dominant loss-of-function mutation of STAT1 (L706S/WT), cells with complete STAT1 deficiency (STAT1<sup>-/-</sup>), and cells from two patients heterozygous for dominant loss-of-function mutations of STAT3 (STAT3<sup>+/-1</sup> and STAT3<sup>+/-2</sup>). Cells were left nonstimulated (NS) or stimulated, as indicated, with IFN- $\gamma$ , IFN- $\alpha$ , IL-27, IL-6, and IL-21. pSTAT is an antibody specific for STAT with a phosphorylated tyrosine residue. (I) The nuclear and cytoplasmic fractions of EBV-B cells from a control (WT/WT), a CMCD patient (R274Q/WT), a heterozygous patient with a dominant loss-of-function mutation of STAT1 (L706S/WT) and a patient with complete STAT1 deficiency (<sup>-/-</sup>) stimulated with IFN- $\gamma$  and IFN- $\alpha$  were tested for the presence of phosphorylated STAT1 and STAT1 by WB. Antibodies directed against GAPDH and Lamin B1 were used to normalize the amount of cytoplasmic and nuclear proteins, respectively. The experiment was performed twice.

Moreover, only very small amounts of IL-17A, IL-17F, and IL-22 were secreted by freshly prepared leukocytes after ex vivo stimulation with PMA and ionomycin ( $P < 8.10^{-3}$ ), as shown by ELISA (Fig. 4, C–E). In contrast, the amounts of secreted IL-17A, IL-17F, and IL-22 were normal in patients heterozygous or homozygous for loss-of-function or hypomorphic STAT1 mutations (Fig. 4, C–E). Interestingly, in all assays, the proportions of IL-17A- and IL-22-producing

T cells and the amounts of IL-17A, IL-17F, and IL-22 secreted were smallest for the four patients with the most apparently severe clinical phenotype (Fig. 4, A–E and not depicted).

After the culture of PBMCs in vitro in the presence of various cytokines, including IL-6, TGF- $\beta$ , IL-1 $\beta$ , and IL-23, the proportion of IL-17A- and IL-22-producing T cell blasts remained significantly lower ( $P < 10^{-4}$ ) in CMCD patients carrying STAT1 mutations than in controls (Fig. S4, A and B; and not depicted). In contrast, the proportions of IL-17A- and IL-22-producing T cell blasts were normal in patients with loss-of-function STAT1 mutations (Fig. S4, A and B; and not depicted). The amounts of IL-17A, IL-17F, and IL-22 in the supernatant of T cell blasts stimulated with PMA and ionomycin after culture in vitro were also significantly lower in patients with STAT1 mutations and CMCD ( $P < 4.10^{-4}$ ; Fig. S4, C–E; and not depicted). In contrast, patients with loss-of-function mutant STAT1 alleles displayed normal levels of cytokine secretion (Fig. S4, C–E; and not depicted). Finally, levels of IL-12p70 and

IL-12p40 production by whole blood stimulated with IFN- $\gamma$  were higher in CMCD patients bearing gain-of-function *STAT1* alleles than in patients bearing loss-of-function *STAT1* alleles and healthy controls (Fig. 4 F and not depicted). Thus, patients with familial or sporadic AD CMCD heterozygous for mutations affecting the coiled-coil domain of *STAT1*, including the dominant gain-of-function R274Q mutant allele, displayed lower levels of IL-17 cytokine production by peripheral T cells, providing a molecular mechanism for the disease.

## DISCUSSION

We have shown that several germline missense mutations affecting the coiled-coil domain of *STAT1* may cause sporadic and familial AD CMCD. The underlying mechanism involves a gain of *STAT1* phosphorylation caused by the loss of nuclear dephosphorylation, resulting in a gain-of-function of GAF in response to various cytokines. Impaired dephosphorylation may not be the only mechanism influencing the impact of these mutations on the transcription of *STAT1* target genes, as these mutations may also affect other processes, such as the dimerization of unphosphorylated *STAT1*. Moreover,

the gain-of-function, which manifests itself in terms of DNA-binding activity, reporter gene induction, and target gene induction, may not necessarily increase the transcription of all target genes, possibly even resulting in the repression of some genes. In addition, the various *STAT1* mutations, although they all affect the coiled-coil domain and are probably all loss-of-dephosphorylation and gain-of-function, may somewhat differ from each other in terms of their functional impact. The genome-wide impact of these mutations on the transcriptome remains to be assessed in various cell types stimulated with a range of cytokines. In any case, the gain-of-function mutant *STAT1* alleles were dominant for GAF activation in all cell types tested. They affected cellular responses to various cytokines, including IFN- $\alpha/\beta$ , IFN- $\gamma$ , and IL-27, which predominantly activate *STAT1* over *STAT3*, and IL-6 and IL-21, which predominantly activate *STAT3* over *STAT1*. These mutations probably also strengthen cellular responses to IFN- $\lambda$ . However, they do not seem to affect *STAT1*-containing ISGF-3 activation by IFN- $\alpha/\beta$ , at least in the conditions tested. Moreover, *STAT3* activation by IL-6, IL-21, IL-22, and IL-23 is maintained, suggesting that *STAT3* activation by IL-26 is also intact.

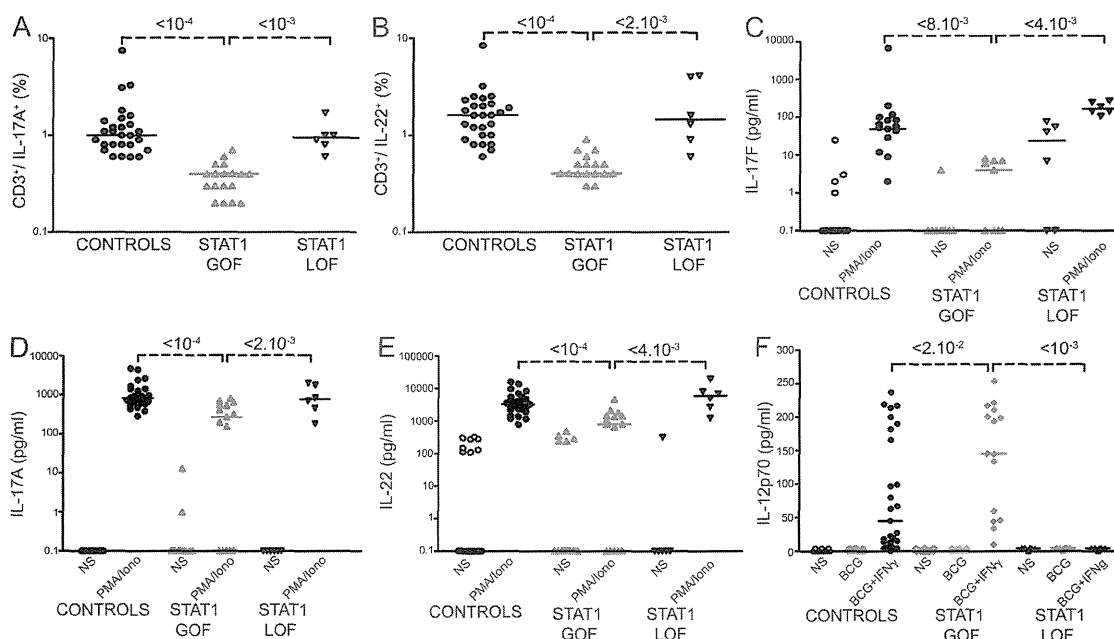


**Figure 4. Impaired development and function of IL-17- and IL-22-producing T cells ex vivo in patients with AD CMCD and *STAT1* mutations.** Each symbol represents a value from a healthy control individual (black circles), a patient bearing a *STAT1* gain-of-function (GOF) allele (red upright triangles), or a patient bearing one or two *STAT1* loss-of-function (LOF) alleles (black upside-down triangles). (A and B) Percentage of CD3<sup>+</sup>/IL-17A<sup>+</sup> (A) and CD3<sup>+</sup>/IL-22<sup>+</sup> (B) cells, as determined by flow cytometry, in nonadherent PBMCs activated by incubation for 12 h with PMA and ionomycin. (C–E) Secretion of IL-17F (C), IL-17A (D) and IL-22 (E) by whole blood cells, as determined by ELISA, in the absence of stimulation (open symbols) and after stimulation with PMA and ionomycin for 48 h (closed symbols). Horizontal bars represent medians. The p-values for the nonparametric Wilcoxon test, between patients with *STAT1* GOF mutations ( $n = 18$ ) and controls ( $n = 28$ ) and patients with *STAT1* LOF mutations ( $n = 6$ ) are indicated. All differences between healthy controls and patients with *STAT1* LOF alleles were not significant. (F) Secretion of IL-12p70 by whole blood cells, as determined by ELISA, in the absence of stimulation (open symbols), after stimulation with BCG (lightly colored symbols), or BCG + IFN- $\gamma$  for 48 h (closed symbols). Horizontal bars represent medians. The p-values for differences between patients with *STAT1* GOF mutations ( $n = 15$ ) and controls ( $n = 23$ ) and patients with *STAT1* LOF mutations ( $n = 6$ ) are indicated and were calculated in nonparametric Wilcoxon tests. All experiments were performed at least two times independently.

The mutant *STAT1* alleles described herein enhance cellular responses to cytokines such as IFN- $\alpha/\beta$ , IFN- $\gamma$ , and IL-27, which potently inhibit the development of IL-17-producing T cells via STAT1 (Batten et al., 2006; Yoshimura et al., 2006; Stumhofer et al., 2006; Amadi-Obi et al., 2007; Feng et al., 2008; Kimura et al., 2008; Tanaka et al., 2008; Chen et al., 2009; Ramgolam et al., 2009; Crabé et al., 2009; Diveu et al., 2009; El-behi et al., 2009; Guzzo et al., 2010; Villarino et al., 2010; Liu and Rohowsky-Kochan, 2011). These mutant alleles also increase cellular responses to IL-6 and IL-21, which normally induce IL-17-producing T cells via STAT3 rather than STAT1 (Hirahara et al., 2010). Enhanced STAT1-dependent cellular responses to these two groups of cytokines probably impair the development of IL-17-producing T cells. It remains unclear whether this mechanism predominantly involves IL-17-inhibiting cytokines (IFN- $\alpha/\beta$ , IFN- $\gamma$ , and IL-27), either individually or in combination. The available data from the mouse model suggest that IL-27 is the most potent of the three inhibitors. There is also evidence that these cytokines inhibit IL-17-producing T cell development in humans (Ramgolam et al., 2009; Liu and Rohowsky-Kochan, 2011). Enhanced STAT1 and GAF activation in response to the IL-17 inducers IL-6 and IL-21, and perhaps IL-23, may also play a key role in disease, by antagonizing STAT3 responses. The effect of the aryl hydrocarbon receptor on IL-17 T cell development might also be enhanced by gain-of-function *STAT1* alleles (Kimura et al., 2008). Moreover, enhanced STAT1 activity downstream from IL-22 and IL-26 in cells, not detected in our study, might also contribute to the CMCD phenotype. Finally, thyroid autoimmunity in eight patients and systemic lupus erythematosus in another patient in our series probably resulted from the enhancement of IFN- $\alpha/\beta$  responses, as such autoimmunity is a frequent adverse effect of treatment with recombinant IFN- $\alpha$  or IFN- $\beta$  (Oppenheim et al., 2004; Selmi et al., 2006). Importantly, no autoantibodies against IL-17A, IL-17F, or IL-22 were detected in the patients' serum (Table I and unpublished data).

Remarkably, germline mutations in human *STAT1* underlie susceptibility to three different types of infectious disease: mycobacterial diseases, viral diseases, and CMC. Patients bearing *STAT1* mutations and displaying mycobacterial and/or viral disease do not suffer from CMC, and the patients with CMCD caused by other *STAT1* alleles described here present no mycobacterial or viral disease. The pathogenic mechanisms involved are clearly different, with loss-of-function mutations in *STAT1* underlying mycobacterial and viral diseases (Dupuis et al., 2001, 2003; Chappier et al., 2006b, 2009; Kong et al., 2010; Averbuch et al., 2011; Kristensen et al., 2011). Human AR *STAT1* deficiency impairs cellular responses to IFN- $\alpha/\beta$ , IFN- $\gamma$ , IFN- $\lambda$ , and IL-27 (Dupuis et al., 2003; Chappier et al., 2006b, 2009; Kong et al., 2010; Kristensen et al., 2011). Viral diseases probably result from impaired IFN- $\alpha/\beta$  and, perhaps, IFN- $\lambda$  immunity, although impaired IFN- $\gamma$  and IL-27 immunity may also contribute to the phenotype. Patients with AD MSMD, heterozygous for loss-of-function dominant-negative mutations of *STAT1*,

suffer from mycobacterial disease caused by the impairment of IFN- $\gamma$  immunity (Chappier et al., 2006a; Dupuis et al., 2001). Overall, mutations impairing STAT1 function confer AD or AR susceptibility to intracellular agents, through the impairment of IFN- $\alpha/\beta$  (viral diseases) and/or IFN- $\gamma$  immunity (mycobacterial diseases). In contrast, the gain-of-function *STAT1* mutations reported here confer AD CMCD because of the enhancement of STAT1-mediated cellular responses to STAT1-dependent repressors and STAT3-dependent inducers of IL-17-producing T cells. These studies neatly demonstrate that severe infectious diseases in otherwise healthy patients may be subject to genetic determinism (Casanova and Abel, 2005, 2007; Alcaïs et al., 2009, 2010). They also highlight the profoundly different effects that germline mutations in the same human gene may have, resulting in different infectious diseases through different molecular and cellular mechanisms.

## MATERIALS AND METHODS

### Massively parallel sequencing

DNA (3  $\mu$ g) extracted from EBV-B cells from the patient was sheared with a S2 Ultrasonicator (Covaris). An adapter-ligated library was prepared with the Paired-End Genomic DNA Sample Prep kit (Illumina). The SureSelect Human All Exon kit (Agilent Technologies) was then used for exome capture. Single-end sequencing was performed on a Genome Analyzer IIX (Illumina), generating 72-base reads.

### Sequence alignment, variant calling, and annotation

BWA aligner (Li and Durbin, 2009) was used to align the sequences obtained with the human genome reference sequence (hg18 build). Downstream processing was performed with the Genome analysis toolkit (GATK; McKenna et al., 2010), SAMtools (Li et al., 2009), and Picard Tools (<http://picard.sourceforge.net>). Substitution calls were made with a GATK UnifiedGenotyper, whereas indel calls were made with a GATK IndelGenotyperV2. All calls with a read coverage  $\leq 2x$  and a Phred-scaled SNP quality of  $\leq 20$  were filtered out. All the variants were annotated with annotation software that was developed in-house. The data were further analyzed with sequence analysis software that had been developed in-house (SQL database query-driven system).

### Molecular genetics

EBV-B cells and the *STAT1*-deficient cell line U3C were cultured as previously described (Chappier et al., 2006a). Primary fibroblasts were cultured in DME supplemented with 10% fetal calf serum. Cells were stimulated with the indicated doses (in IU/ml or ng/ml) of IFN- $\gamma$  (Imukin; Boehringer Ingelheim), IFN- $\alpha 2b$  (IntronA; Schering-Plough), IL-27 (R&D Systems), IL-21 (R&D Systems), IL-22 (R&D Systems), IL-23 (R&D Systems), and IL-6 (R&D Systems). Genomic DNA and total RNA were extracted from cell lines and fresh blood cells, as previously described (Chappier et al., 2006a). Genomic DNA was amplified with specific primers encompassing exons 6–10 of *STAT1* (available upon request), sequenced with the Big Dye Terminator cycle sequencing kit (Applied Biosystems), and analyzed on an ABI Prism 3730 (Applied Biosystems). We used the various alleles of *STAT1* in the pcDNA3 *STAT1*-V5 vector (Chappier et al., 2006a; Kong et al., 2010). We generated the various *STAT1* mutations by site-directed mutagenesis (QuikChange Site-Directed Mutagenesis kit; Stratagene) with the mismatched primers listed in Table S4. U3C cells were harvested by trypsin treatment 24 h before transfection and replated at a density of  $2.5 \times 10^5$  cells/ml in 6-well plates. Plasmid DNA (5  $\mu$ g per plate) carrying the WT or all the various mutant *STAT1* alleles was used for cell transfection with the Calcium Phosphate Transfection kit (Invitrogen).

### Luciferase reporter assay

U3C cells were dispensed into 96-well plates ( $1 \times 10^4$ /well) and transfected with reporter plasmids (Cignal GAS and ISRE Reporter Assay kit;

SABiosciences) and plasmids carrying the various alleles of *STAT1* or a mock vector, in the presence of Lipofectamine LTX (Invitrogen). 6 h after transfection, the cells were transferred back into medium containing 10% FBS and cultured for 24 h. The transfectants were then stimulated with IFN- $\gamma$  (500 and 1,000 IU/ml), IL-27 (20 and 100 ng/ml), and IFN- $\alpha$  (500, 1,000, and 5,000 IU/ml) for 16 h and subjected to luciferase assays with the Dual-Glo luciferase assay system (Promega). Experiments were performed in triplicate and firefly luciferase activity was normalized with respect to *Renilla* luciferase activity. The data are expressed as fold induction with respect to nonstimulated cells.

#### Immunoblot analysis and electrophoretic mobility shift assays

The following optimal stimulation conditions were used. EBV-B or U3C cells were stimulated by incubation for 20 min with 100  $\mu$ g/ml IL-21 or 25 ng of IL-22; 30 min with  $10^3$  or  $10^5$  IU/ml IFN- $\gamma$  and IFN- $\alpha$ ; 15 min with 50 ng/ml IL-6; or 30 min with 50 or 100 ng/ml IL-27. WB was performed as previously described (Dupuis et al., 2003). In brief, cell activation was blocked with cold 1X PBS, cells were lysed in 1% NP-40 lysis buffer, and the proteins were recovered and subjected to SDS-PAGE. We used antibodies directed against phosphorylated STAT1 (pY701; BD), STAT1 (C-24; Santa Cruz Biotechnology), V5 (Invitrogen),  $\alpha$ -tubulin (Santa Cruz Biotechnology), phosphorylated STAT3 (Cell Signaling Technology), lamin B1 (Santa Cruz Biotechnology), GAPDH (Santa Cruz Biotechnology), and STAT3 (Santa Cruz Biotechnology). EMSA was performed as previously described (Chappier et al., 2006a). In brief, cell activation was blocked by incubation with cold 1X PBS, and the cells were gently lysed to remove cytoplasmic proteins while keeping the nucleus intact. We then added nuclear lysis buffer and recovered the nuclear proteins, which were subjected to non-denaturing electrophoresis with radiolabeled GAS (from the FC $\gamma$ R1 promoter: 5'-ATGTATTTCCAGAAA-3') and ISRE (from the ISG15 promoter: 5'-GATCGGAAAGGAAACCGAAACTGAA-3') probes.

#### Staurosporine and pervanadate treatment of cells

We assessed dephosphorylation by stimulating U3C transfectants with  $10^5$  IU/ml IFN- $\gamma$ . The cells were then washed and incubated with 1  $\mu$ M staurosporine in DME for 15, 30, or 60 min. The cells were then lysed with 1% NP-40 lysis buffer, and the proteins recovered were subjected to immunoblot analysis.

Pervanadate was prepared by mixing orthovanadate with H<sub>2</sub>O<sub>2</sub> for 15 min at 22°C. U3C transfectants were treated with pervanadate (0.8 mM orthovanadate and 0.2 mM H<sub>2</sub>O<sub>2</sub>) 5 min before stimulation. They were then stimulated with IFN- $\gamma$  for 20 min. The stimulation was stopped by adding cold 1X PBS. The proteins were recovered and subjected to immunoblot analysis.

#### Extraction of nuclear and cytoplasmic proteins

U3C transfectants or EBV-B cells were stimulated with IFN- $\gamma$  or IFN- $\alpha$  for 20 min and subjected to nuclear and cytoplasmic protein extraction with NE-PER Nuclear and Cytoplasmic Extraction Regents (Thermo Fisher Scientific) according to the manufacturer's protocol.

#### Immunofluorescence staining

Immunofluorescence experiments were performed as previously described (Chappier et al., 2006a). In brief, cells (transfected U3C or SV-40 fibroblasts) were stimulated for the times indicated with 10,000 IU/ml of IFN- $\gamma$ . Cells were then washed with cold PBS and fixed with 4% PFA. The cells were washed and incubated with an antibody against STAT1, which was then detected by incubation with an Alexa Fluor 488-conjugated anti-mouse antibody.

#### T cell blast differentiation and stimulation

PBMCs were recovered by centrifuging blood samples on Ficoll gradients, as previously described (Chappier et al., 2006a). They were then cultivated, at a density of 1 million cells per ml in RPMI supplemented with 10% fetal calf serum and stimulated with phytohemagglutinin (1  $\mu$ g/ml) for 3 d. Cells were then recovered, centrifuged on a Ficoll gradient, cultivated (at a density of 0.2 million cells/ml) to Panserin 401 supplemented with 10% FCS and glutamine 1X, and stimulated with 40 IU/ml IL-2 (Roche). Cells were then

incubated for 30 min with 100 ng/ml IL-23. Activation was stopped by adding 1X cold PBS, and cells were processed for immunoblot analysis.

#### Modeling

Images of the three-dimensional structure of STAT1 (Chen et al., 1998) were generated with the 2002 PyMOL Molecular Graphics System (DeLano Scientific), using PDB accession no. 1BF5.

#### Whole-blood assay of the IL-12-IFN- $\gamma$ circuit

Whole-blood assays were performed as previously described (Feinberg et al., 2004). Heparin-treated blood samples from healthy controls and patients were stimulated in vitro with live *Mycobacterium bovis* BCG (Pasteur) alone or with IFN- $\gamma$  (5,000 IU/ml; Boehringer Ingelheim). Supernatants were collected after 48 h of stimulation, and ELISA were performed with specific antibodies directed against IL-12p40 or IL-12p70, using kits from R&D Systems according to the manufacturer's instructions.

#### Production of IL-17A, IL-17F, and IL-22 by leukocytes

**Cell activation.** IL-17A- and IL-22-producing T cells were evaluated by intracellular staining or by ELISA, as previously described (de Beaucoudrey et al., 2008). In brief, PBMCs were purified by centrifugation on a gradient (Ficoll-Paque PLUS; GE Healthcare) and resuspended in RPMI supplemented with 10% FBS (RPMI/10% FBS; Invitrogen). Adherent monocytes were removed from the PBMC preparation by incubation for 2 h at 37°C, under an atmosphere containing 5% CO<sub>2</sub>.

For ex vivo evaluation of IL-17- and IL-22-producing T cells by flow cytometry, we resuspended  $5 \times 10^6$  nonadherent cells in 5 ml RPMI/10% FBS in 25 cm<sup>2</sup> flasks and stimulated them by incubation with 40 ng/ml PMA (Sigma-Aldrich) and  $10^{-5}$  M ionomycin (Sigma-Aldrich) in the presence of a secretion inhibitor (1  $\mu$ l/ml GolgiPlug; BD) for 12 h.

For evaluation of the IL-17- and IL-22-producing T cell blasts after in vitro differentiation, the nonadherent PBMCs were dispensed into 24-well plates at a density of  $2.5 \times 10^6$  cells/ml in RPMI/10% FBS and activated with 2  $\mu$ g/ml of an antibody directed against CD3 (Orthoclone OKT3; Janssen-Cilag) alone, or together with 5 ng/ml TGF- $\beta$ 1 (240-B; R&D Systems), 20 ng/ml IL-23 (1290-IL; R&D Systems), 50 ng/ml IL-6 (206-IL; R&D Systems), 10 ng/ml IL-1 $\beta$  (201-LB; R&D Systems), or combinations of these four cytokines. After 3 d, the cells were restimulated in the same activation conditions, except that the anti-CD3 antibody was replaced with 40 IU/ml IL-2 (Proleukin i.v.; Chiron). We added 1 ml of the appropriate medium, resuspended the cells by gentle pipetting, and then split the cell suspension from each well into two. Flow cytometry was performed on one of the duplicated wells 2 d later, after stimulation by incubation for 12 h with 40 ng/ml PMA and  $10^{-5}$  M ionomycin in the presence of 1  $\mu$ l/ml GolgiPlug. FACS analysis was performed as described in the following section. The other duplicated well was split into two, with one half left unstimulated and the other stimulated by incubation with 40 ng/ml PMA and  $10^{-5}$  M ionomycin for another 2 d. Supernatants were collected after 48 h of incubation, for ELISA.

**Flow cytometry.** Cells were washed in cold PBS, and surface labeling was achieved by incubating the cells with PE-Cy5-conjugated anti-human CD3 antibody (BD) in PBS/2% FBS for 20 min on ice. Cells were then washed twice with 2% FBS in cold PBS, fixed by incubation with 100  $\mu$ l of BD Cytofix for 30 min on ice, and washed twice with BD Cytoperm (Cytofix/Cytoperm Plus, fixation/permeabilization kit; BD). Cells were then incubated for 1 h on ice with Alexa Fluor 488-conjugated anti-human IL-17A (53-7179-42; eBioscience), PE-conjugated anti-human IL-22 (IC7821P; R&D Systems), or PE-conjugated anti-human IFN- $\gamma$  (IC285P; R&D Systems) antibodies, washed twice with Cytoperm, and analyzed with a FACS-Canto II system (BD).

**ELISA.** IL-17A, IL-17F, and IL-22 levels were determined by ELISA on the supernatants harvested after 48 h of whole-blood stimulation with 40 ng/ml PMA and  $10^{-5}$  M ionomycin, or after in vitro PHA blast differentiation and

48 h of stimulation with 40 ng/ml PMA and  $10^{-5}$  M ionomycin. We used anti-human IL-17A and anti-human IL-22 DuoSet kits (R&D Systems) and the anti-human IL-17F ELISA Ready-SET-GO! set (eBioscience).

**Statistical analysis.** We assessed differences between controls, MSMD patients bearing loss-of-function *STAT1* alleles, and CMCD patients bearing gain-of-function *STAT1* alleles in terms of the percentages of IL-17A- and IL-22-producing T cells, as assessed by flow cytometry, and in terms of the amounts of IL-17A, IL-17F, and IL-22 produced in various stimulation conditions, as assessed by ELISA. We used the nonparametric Wilcoxon test, as implemented in the PROC NPAR1WAY of the SAS software version 9.1 (SAS Institute). For all analyses,  $P < 0.05$  was considered statistically significant.

#### Online supplemental material

Fig. S1 shows that *STAT1*-CMCD mutants are gain-of-function alleles by loss of nuclear dephosphorylation. Fig. S2 is a schematic representation of the cytokines and transcription factors directing the development of naive CD4 cells into IL-17-producing T cells. Fig. S3 shows the normal response of CMCD patient cells to IFN- $\alpha$  in terms of ISGF3 activation, to IFN- $\gamma$  in terms of *STAT1* nuclear translocation; and to IL-23 and IL-22 in terms of p*STAT3*. Fig. S4 shows impaired *in vitro* differentiation of IL-17- and IL-22-producing T cell blasts in patients with CMCD and gain-of-function *SATA1* mutations. Table S1 shows novel coding heterozygous variants found by whole-exome sequencing in the 6 different patients. Table S2 shows novel coding heterozygous variants found by whole-exome sequencing within genes shared by more than one patient. Table S3 lists conservation and predictions on the function of the mutant *STAT1* alleles associated with CMCD. Table S4 lists the *STAT1* GOF mutation created, and the pair of primers used. Online supplemental material is available at <http://www.jem.org/cgi/content/full/jem.20110958/DC1>.

We thank the members of the laboratory for helpful discussions; Yelena Nemiroskaya, Eric Anderson, Martine Courat, and Michele N'Guyen for secretarial assistance; and Tony Leclerc and Tiffany Nivare for technical assistance. We also thank Alekszandra Barsony, Dmitriy Samarin, Fedir Lapij, Maxim Vodyanik, Marcela Moncada Velez, Bertrand Boisson, and Astrid Research, Inc.

This work was supported by grants from Institut National de la Santé et de la Recherche Médicale, University Paris Descartes, the Rockefeller University, the Rockefeller University CTSA grant number 5UL1RRO24143-04, the St. Giles Foundation, and the Candidoser Association awarded to Jean-Laurent Casanova. Janine Reichenbach was supported by the Gebert Ruff Stiftung, program "Rare Diseases - New Approaches"; Ellen Renner by the DFG RE2799/3-1 and a Fritz-Thyssen research foundation grant (Az. 10.07.1.159). Support was also provided by TÁMOP 4.2.1./B-09/1/KONV-2010-0007 and TÁMOP 4.2.2-08/1-2008-0015 grants to László Maródi and LMU Munich F6FoLe grant #680/658. Sophie Cypowj was supported by the AXA Research Fund, and Xiaofei Kong by the Choh-Hao Li Memorial Fund Scholar award and the Shanghai Educational Development Foundation. We have all the approvals and authorizations required for this study (Necker IRB, Paris, 1995 and Rockefeller IRB, New York, 2008).

The authors state no conflict of interest.

Submitted: 11 May 2011

Accepted: 22 June 2011

#### REFERENCES

- Adzhubei, I.A., S. Schmidt, L. Peshkin, V.E. Ramensky, A. Gerasimova, P. Bork, A.S. Kondrashov, and S.R. Sunyaev. 2010. A method and server for predicting damaging missense mutations. *Nat. Methods*. 7:248–249. doi:10.1038/nmeth0410-248
- Alcaïs, A., L. Abel, and J.L. Casanova. 2009. Human genetics of infectious diseases: between proof of principle and paradigm. *J. Clin. Invest.* 119:2506–2514. doi:10.1172/JCI38111
- Alcaïs, A., L. Quintana-Murci, D.S. Thaler, E. Schurr, L. Abel, and J.L. Casanova. 2010. Life-threatening infectious diseases of childhood: single-gene inborn errors of immunity? *Ann. N.Y. Acad. Sci.* 1214:18–33. doi:10.1111/j.1749-6632.2010.05834.x
- Amadi-Obi, A., C.R. Yu, X. Liu, R.M. Mahdi, G.L. Clarke, R.B. Nussenblatt, I. Gery, Y.S. Lee, and C.E. Egwuagu. 2007. TH17 cells contribute to
- uveitis and scleritis and are expanded by IL-2 and inhibited by IL-27/STAT1. *Nat. Med.* 13:711–718. doi:10.1038/nm1585
- Atkinson, T.P., A.A. Schäffer, B. Grimbacher, H.W. Schroeder Jr., C. Woellner, C.S. Zerbe, and J.M. Puck. 2001. An immune defect causing dominant chronic mucocutaneous candidiasis and thyroid disease maps to chromosome 2p in a single family. *Am. J. Hum. Genet.* 69:791–803. doi:10.1086/323611
- Averbuch, D., A. Chappier, S. Boisson-Dupuis, J.L. Casanova, and D. Engelhard. 2011. The clinical spectrum of patients with deficiency of Signal Transducer and Activator of Transcription-1. *Pediatr. Infect. Dis. J.* 30:352–355.
- Batten, M., J. Li, S. Yi, N.M. Kljavin, D.M. Danilenko, S. Lucas, J. Lee, F.J. de Sauvage, and N. Ghilardi. 2006. Interleukin 27 limits autoimmune encephalomyelitis by suppressing the development of interleukin 17-producing T cells. *Nat. Immunol.* 7:929–936. doi:10.1038/ni1375
- Bentur, L., E. Nisbet-Brown, H. Levison, and C.M. Roifman. 1991. Lung disease associated with IgG subclass deficiency in chronic mucocutaneous candidiasis. *J. Pediatr.* 118:82–86. doi:10.1016/S0022-3476(05)81852-9
- Bolze, A., M. Byun, D. McDonald, N.V. Morgan, A. Abhyankar, L. Premkumar, A. Puel, C.M. Bacon, F. Rieux-Laucat, K. Pang, et al. 2010. Whole-exome-sequencing-based discovery of human FADD deficiency. *Am. J. Hum. Genet.* 87:873–881. doi:10.1016/j.ajhg.2010.10.028
- Braunstein, J., S. Brutsaert, R. Olson, and C. Schindler. 2003. STATs dimerize in the absence of phosphorylation. *J. Biol. Chem.* 278:34133–34140. doi:10.1074/jbc.M304531200
- Byun, M., A. Abhyankar, V. Lelarge, S. Plancoulaine, A. Palanduz, L. Telhan, B. Boisson, C. Picard, S. Dewell, C. Zhao, et al. 2010. Whole-exome sequencing-based discovery of *STIM1* deficiency in a child with fatal classic Kaposi sarcoma. *J. Exp. Med.* 207:2307–2312. doi:10.1084/jem.20101597
- Casanova, J.L., and L. Abel. 2005. Inborn errors of immunity to infection: the rule rather than the exception. *J. Exp. Med.* 202:197–201. doi:10.1084/jem.20050854
- Casanova, J.L., and L. Abel. 2007. Primary immunodeficiencies: a field in its infancy. *Science*. 317:617–619. doi:10.1126/science.1142963
- Chappier, A., S. Boisson-Dupuis, E. Jouanguy, G. Vogt, J. Feinberg, A. Prochnicka-Chalouf, A. Casrouge, K. Yang, C. Soudais, C. Fieschi, et al. 2006a. Novel *STAT1* alleles in otherwise healthy patients with mycobacterial disease. *PLoS Genet.* 2:e131. doi:10.1371/journal.pgen.0020131
- Chappier, A., R.F. Wynn, E. Jouanguy, O. Filipe-Santos, S. Zhang, J. Feinberg, K. Hawkins, J.L. Casanova, and P.D. Arkwright. 2006b. Human complete Stat-1 deficiency is associated with defective type I and II IFN responses *in vitro* but immunity to some low virulence viruses *in vivo*. *J. Immunol.* 176:5078–5083.
- Chappier, A., X.F. Kong, S. Boisson-Dupuis, E. Jouanguy, D. Averbuch, J. Feinberg, S.Y. Zhang, J. Bustamante, G. Vogt, J. Lejeune, et al. 2009. A partial form of recessive *STAT1* deficiency in humans. *J. Clin. Invest.* 119:1502–1514. doi:10.1172/JCI37083
- Chen, X., U. Vinkemeier, Y. Zhao, D. Jeruzalmi, J.E. Darnell Jr., and J. Kuriyan. 1998. Crystal structure of a tyrosine phosphorylated *STAT-1* dimer bound to DNA. *Cell*. 93:827–839. doi:10.1016/S0092-8674(00)81443-9
- Chen, M., G. Chen, H. Nie, X. Zhang, X. Niu, Y.C. Zang, S.M. Skinner, J.Z. Zhang, J.M. Killian, and J. Hong. 2009. Regulatory effects of IFN- $\beta$  on production of osteopontin and IL-17 by CD4+ T Cells in MS. *Eur. J. Immunol.* 39:2525–2536. doi:10.1002/eji.200838879
- Crabé, S., A. Guay-Giroux, A.J. Tormo, D. Duluc, R. Lissilaa, F. Guilhot, U. Mavoungou-Bigouagou, F. Lefouili, I. Cognet, W. Ferlin, et al. 2009. The IL-27 p28 subunit binds cytokine-like factor 1 to form a cytokine regulating NK and T cell activities requiring IL-6R for signaling. *J. Immunol.* 183:7692–7702. doi:10.4049/jimmunol.0901464
- de Beaucoudrey, L., A. Puel, O. Filipe-Santos, A. Cobat, P. Ghandil, M. Chrabieh, J. Feinberg, H. von Bernuth, A. Samarina, L. Jannié, et al. 2008. Mutations in *STAT3* and *IL12RB1* impair the development of human IL-17-producing T cells. *J. Exp. Med.* 205:1543–1550. doi:10.1084/jem.20080321
- de Beaucoudrey, L., A. Samarina, J. Bustamante, A. Cobat, S. Boisson-Dupuis, J. Feinberg, S. Al-Muhsen, L. Jannié, Y. Rose, M. de Suremain, et al. 2010. Revisiting human IL-12R $\beta$ 1 deficiency: a survey of 141 patients from 30 countries. *Medicine*. 89:381–402. doi:10.1097/MD.0b013e3181fdd832

- Diveu, C., M.J. McGeachy, K. Boniface, J.S. Stumhofer, M. Sathe, B. Joyce-Shaikh, Y. Chen, C.M. Tato, T.K. McClanahan, R. de Waal Malefyt, et al. 2009. IL-27 blocks ROR $\gamma$ c expression to inhibit lineage commitment of Th17 cells. *J. Immunol.* 182:5748–5756. doi:10.4049/jimmunol.0801162
- Donnelly, R.P., F. Sheikh, H. Dickensheets, R. Savan, H.A. Young, and M.R. Walter. 2010. Interleukin-26: an IL-10-related cytokine produced by Th17 cells. *Cytokine Growth Factor Rev.* 21:393–401. doi:10.1016/j.cytogfr.2010.09.001
- Dupuis, S., C. Dargemont, C. Fieschi, N. Thomassin, S. Rosenzweig, J. Harris, S.M. Holland, R.D. Schreiber, and J.L. Casanova. 2001. Impairment of mycobacterial but not viral immunity by a germline human STAT1 mutation. *Science.* 293:300–303. doi:10.1126/science.1061154
- Dupuis, S., E. Jouanguy, S. Al-Hajjar, C. Fieschi, I.Z. Al-Mohsen, S. Al-Jumaah, K. Yang, A. Chaggier, C. Eidenschenk, P. Eid, et al. 2003. Impaired response to interferon-alpha/beta and lethal viral disease in human STAT1 deficiency. *Nat. Genet.* 33:388–391. doi:10.1038/ng1097
- El-behi, M., B. Ciric, S. Yu, G.X. Zhang, D.C. Fitzgerald, and A. Rostami. 2009. Differential effect of IL-27 on developing versus committed Th17 cells. *J. Immunol.* 183:4957–4967. doi:10.4049/jimmunol.0900735
- Eyerich, K., S. Foerster, S. Rombold, H.P. Seidl, H. Behrendt, H. Hofmann, J. Ring, and C. Traidl-Hoffmann. 2008. Patients with chronic mucocutaneous candidiasis exhibit reduced production of Th17-associated cytokines IL-17 and IL-22. *J. Invest. Dermatol.* 128:2640–2645. doi:10.1038/jid.2008.139
- Feinberg, J., C. Fieschi, R. Doffinger, M. Feinberg, T. Leclerc, S. Boisson-Dupuis, C. Picard, J. Bustamante, A. Chaggier, O. Filipe-Santos, et al. 2004. Bacillus Calmette Guerin triggers the IL-12/IFN-gamma axis by an IRAK-4- and NEMO-dependent, non-cognate interaction between monocytes, NK, and T lymphocytes. *Eur. J. Immunol.* 34:3276–3284. doi:10.1002/eji.200425221
- Feng, G., W. Gao, T.B. Strom, M. Oukka, R.S. Francis, K.J. Wood, and A. Bushnell. 2008. Exogenous IFN-gamma ex vivo shapes the alloreactive T-cell repertoire by inhibition of Th17 responses and generation of functional Foxp3<sup>+</sup> regulatory T cells. *Eur. J. Immunol.* 38:2512–2527. doi:10.1002/eji.200838411
- Filipe-Santos, O., J. Bustamante, A. Chaggier, G. Vogt, L. de Beaucoudrey, J. Feinberg, E. Jouanguy, S. Boisson-Dupuis, C. Fieschi, C. Picard, and J.L. Casanova. 2006. Inborn errors of IL-12/23- and IFN-gamma-mediated immunity: molecular, cellular, and clinical features. *Semin. Immunol.* 18:347–361. doi:10.1016/j.smim.2006.07.010
- Germain, M., M. Gourdeau, and J. Hébert. 1994. Case report: familial chronic mucocutaneous candidiasis complicated by deep candida infection. *Am. J. Med. Sci.* 307:282–283. doi:10.1097/0000441-199404000-00008
- Glocker, E.O., A. Hennigs, M. Nabavi, A.A. Schäffer, C. Woellner, U. Salzer, D. Pfeifer, H. Veecken, K. Warnatz, F. Tahami, et al. 2009. A homozygous CARD9 mutation in a family with susceptibility to fungal infections. *N. Engl. J. Med.* 361:1727–1735. doi:10.1056/NEJMoa0810719
- Guzzo, C., N.F. Che Mat, and K. Gee. 2010. Interleukin-27 induces a STAT1/3- and NF-kappaB-dependent proinflammatory cytokine profile in human monocytes. *J. Biol. Chem.* 285:24404–24411. doi:10.1074/jbc.M110.112599
- Herrod, H.G. 1990. Chronic mucocutaneous candidiasis in childhood and complications of non-Candida infection: a report of the Pediatric Immunodeficiency Collaborative Study Group. *J. Pediatr.* 116:377–382. doi:10.1016/S0022-3476(05)82824-0
- Hirahara, K., K. Ghoreschi, A. Laurence, X.P. Yang, Y. Kanno, and J.J. O'Shea. 2010. Signal transduction pathways and transcriptional regulation in Th17 cell differentiation. *Cytokine Growth Factor Rev.* 21:425–434. doi:10.1016/j.cytogfr.2010.10.006
- Hoshino, A., S. Saint Fleur, and H. Fujii. 2006. Regulation of Stat1 protein expression by phenylalanine 172 in the coiled-coil domain. *Biochem. Biophys. Res. Commun.* 346:1062–1066. doi:10.1016/j.bbrc.2006.06.026
- Hunter, C.A. 2005. New IL-12-family members: IL-23 and IL-27, cytokines with divergent functions. *Nat. Rev. Immunol.* 5:521–531. doi:10.1038/nri1648
- Kastelein, R.A., C.A. Hunter, and D.J. Cua. 2007. Discovery and biology of IL-23 and IL-27: related but functionally distinct regulators of inflammation. *Annu. Rev. Immunol.* 25:221–242. doi:10.1146/annurev.immunol.22.012703.104758
- Kimura, A., T. Naka, K. Nohara, Y. Fujii-Kuriyama, and T. Kishimoto. 2008. Aryl hydrocarbon receptor regulates Stat1 activation and participates in the development of Th17 cells. *Proc. Natl. Acad. Sci. USA.* 105:9721–9726. doi:10.1073/pnas.0804231105
- Kirkpatrick, C.H. 2001. Chronic mucocutaneous candidiasis. *Pediatr. Infect. Dis. J.* 20:197–206. doi:10.1097/00006454-200102000-00017
- Kisand, K., A.S. Bøe Wolff, K.T. Podkrajsek, L. Tserel, M. Link, K.V. Kisand, E. Ersvaer, J. Perheentupa, M.M. Erichsen, N. Bratanic, et al. 2010. Chronic mucocutaneous candidiasis in APECED or thymoma patients correlates with autoimmunity to Th17-associated cytokines. *J. Exp. Med.* 207:299–308. doi:10.1084/jem.20091669
- Kishimoto, T. 2005. Interleukin-6: from basic science to medicine—40 years in immunology. *Annu. Rev. Immunol.* 23:1–21. doi:10.1146/annurev.immunol.23.021704.115806
- Kong, X.F., M. Ciancanelli, S. Al-Hajjar, L. Alsina, T. Zumwalt, J. Bustamante, J. Feinberg, M. Audry, C. Prando, V. Bryant, et al. 2010. A novel form of human STAT1 deficiency impairing early but not late responses to interferons. *Blood.* 116:5895–5906. doi:10.1182/blood-2010-04-280586
- Kristensen, I.A., J.E. Veirum, B.K. Møller, and M. Christiansen. 2011. Novel STAT1 Alleles in a Patient with Impaired Resistance to Mycobacteria. *J. Clin. Immunol.* 31:265–271. doi:10.1007/s10875-010-9480-8
- Levy, D.E., and J.E. Darnell Jr. 2002. Stats: transcriptional control and biological impact. *Nat. Rev. Mol. Cell Biol.* 3:651–662. doi:10.1038/nrm909
- Li, H., and R. Durbin. 2009. Fast and accurate short read alignment with Burrows-Wheeler transform. *Bioinformatics.* 25:1754–1760.
- Lilic, D. 2002. New perspectives on the immunology of chronic mucocutaneous candidiasis. *Curr. Opin. Infect. Dis.* 15:143–147. doi:10.1097/00001432-200204000-00007
- Liu, H., and C. Rohowsky-Kochan. 2011. Interleukin-27-Mediated Suppression of Human Th17 Cells Is Associated with Activation of STAT1 and Suppressor of Cytokine Signaling Protein 1. *J. Interferon Cytokine Res.* 31:459–469. doi:10.1089/jir.2010.0115
- Ma, C.S., G.Y. Chew, N. Simpson, A. Priyadarshi, M. Wong, B. Grimbacher, D.A. Fulcher, S.G. Tangye, and M.C. Cook. 2008. Deficiency of Th17 cells in hyper IgE syndrome due to mutations in STAT3. *J. Exp. Med.* 205:1551–1557. doi:10.1084/jem.20080218
- McKenna, A., M. Hanna, E. Banks, A. Sivachenko, K. Cibulskis, A. Kernysky, K. Garimella, D. Altshuler, S. Gabriel, M. Daly, and M.A. DePristo. 2010. The Genome Analysis Toolkit: a MapReduce framework for analyzing next-generation DNA sequencing data. *Genome Res.* 20:1297–1303.
- Mertens, C., M. Zhong, R. Krishnaraj, W. Zou, X. Chen, and J.E. Darnell Jr. 2006. Dephosphorylation of phosphotyrosine on STAT1 dimers requires extensive spatial reorientation of the monomers facilitated by the N-terminal domain. *Genes Dev.* 20:3372–3381. doi:10.1101/gad.1485406
- Milner, J.D., J.M. Brenchley, A. Laurence, A.F. Freeman, B.J. Hill, K.M. Elias, Y. Kanno, C. Spalding, H.Z. Elloumi, M.L. Paulson, et al. 2008. Impaired T(H)17 cell differentiation in subjects with autosomal dominant hyper-IgE syndrome. *Nature.* 452:773–776. doi:10.1038/nature06764
- Minegishi, Y. 2009. Hyper-IgE syndrome. *Curr. Opin. Immunol.* 21:487–492. doi:10.1016/j.coi.2009.07.013
- Minegishi, Y., M. Saito, M. Nagasawa, H. Takada, T. Hara, S. Tsuchiya, K. Agematsu, M. Yamada, N. Kawamura, T. Ariga, et al. 2009. Molecular explanation for the contradiction between systemic Th17 defect and localized bacterial infection in hyper-IgE syndrome. *J. Exp. Med.* 206:1291–1301. doi:10.1084/jem.20082767
- Ng, S.B., K.J. Buckingham, C. Lee, A.W. Bigham, H.K. Tabor, K.M. Dent, C.D. Huff, P.T. Shannon, E.W. Jabs, D.A. Nickerson, et al. 2010. Exome sequencing identifies the cause of a mendelian disorder. *Nat. Genet.* 42:30–35. doi:10.1038/ng.499
- Oppenheim, Y., Y. Ban, and Y. Tomer. 2004. Interferon induced Autoimmune Thyroid Disease (AITD): a model for human autoimmunity. *Autoimmun. Rev.* 3:388–393. doi:10.1016/j.autrev.2004.03.003
- Ouyang, W., S. Rutz, N.K. Crellin, P.A. Valdez, and S.G. Hymowitz. 2011. Regulation and functions of the IL-10 family of cytokines in

- inflammation and disease. *Annu. Rev. Immunol.* 29:71–109. doi:10.1146/annurev-immunol-031210-101312
- Puel, A., R. Döfninger, A. Natividad, M. Chrabieh, G. Barcenás-Morales, C. Picard, A. Cobat, M. Ouachée-Chardin, A. Toulon, J. Bustamante, et al. 2010a. Autoantibodies against IL-17A, IL-17F, and IL-22 in patients with chronic mucocutaneous candidiasis and autoimmune polyendocrine syndrome type I. *J. Exp. Med.* 207:291–297. doi:10.1084/jem.20091983
- Puel, A., C. Picard, S. Cypowij, D. Lilic, L. Abel, and J.L. Casanova. 2010b. Inborn errors of mucocutaneous immunity to *Candida albicans* in humans: a role for IL-17 cytokines? *Curr. Opin. Immunol.* 22:467–474. doi:10.1016/j.coi.2010.06.009
- Puel, A., S. Cypowij, J. Bustamante, J.F. Wright, L. Liu, H.K. Lim, M. Migaud, L. Israel, M. Chrabieh, M. Audry, et al. 2011. Chronic mucocutaneous candidiasis in humans with inborn errors of interleukin-17 immunity. *Science*. 332:65–68. doi:10.1126/science.1200439
- Ramgolam, V.S., Y. Sha, J. Jin, X. Zhang, and S. Markovic-Plese. 2009. IFN- $\beta$  inhibits human Th17 cell differentiation. *J. Immunol.* 183:5418–5427. doi:10.4049/jimmunol.0803227
- Renner, E.D., S. Rylaarsdam, S. Anover-Sombke, A.L. Rack, J. Reichenbach, J.C. Carey, Q. Zhu, A.F. Jansson, J. Barboza, L.F. Schimke, et al. 2008. Novel signal transducer and activator of transcription 3 (STAT3) mutations, reduced T(H)17 cell numbers, and variably defective STAT3 phosphorylation in hyper-IgE syndrome. *J. Allergy Clin. Immunol.* 122:181–187. doi:10.1016/j.jaci.2008.04.037
- Sabat, R. 2010. IL-10 family of cytokines. *Cytokine Growth Factor Rev.* 21:315–324. doi:10.1016/j.cytogfr.2010.11.001
- Selmi, C., A. Lleo, M. Zuin, M. Podda, L. Rossaro, and M.E. Gershwin. 2006. Interferon alpha and its contribution to autoimmunity. *Curr. Opin. Investig. Drugs*. 7:451–456.
- Shama, S.K., and C.H. Kirkpatrick. 1980. Dermatophytosis in patients with chronic mucocutaneous candidiasis. *J. Am. Acad. Dermatol.* 2:285–294. doi:10.1016/S0190-9622(80)80040-5
- Spolski, R., and W.J. Leonard. 2008. Interleukin-21: basic biology and implications for cancer and autoimmunity. *Annu. Rev. Immunol.* 26:57–79. doi:10.1146/annurev-immunol.26.021607.090316
- Stumhofer, J.S., A. Laurence, E.H. Wilson, E. Huang, C.M. Tato, L.M. Johnson, A.V. Villarino, Q. Huang, A. Yoshimura, D. Sehly, et al. 2006. Interleukin 27 negatively regulates the development of interleukin 17-producing T helper cells during chronic inflammation of the central nervous system. *Nat. Immunol.* 7:937–945. doi:10.1038/ni1376
- Tanaka, K., K. Ichiyama, M. Hashimoto, H. Yoshida, T. Takimoto, G. Takaesu, T. Torisu, T. Hanada, H. Yasukawa, S. Fukuyama, et al. 2008. Loss of suppressor of cytokine signaling 1 in helper T cells leads to defective Th17 differentiation by enhancing antagonistic effects of IFN- $\gamma$  on STAT3 and Smads. *J. Immunol.* 180:3746–3756.
- Villarino, A.V., E. Gallo, and A.K. Abbas. 2010. STAT1-activating cytokines limit Th17 responses through both T-bet-dependent and -independent mechanisms. *J. Immunol.* 185:6461–6471. doi:10.4049/jimmunol.1001343
- Yoshimura, T., A. Takeda, S. Hamano, Y. Miyazaki, I. Kinjyo, T. Ishibashi, A. Yoshimura, and H. Yoshida. 2006. Two-sided roles of IL-27: induction of Th1 differentiation on naive CD4<sup>+</sup> T cells versus suppression of pro-inflammatory cytokine production including IL-23-induced IL-17 on activated CD4<sup>+</sup> T cells partially through STAT3-dependent mechanism. *J. Immunol.* 177:5377–5385.
- Zhong, M., M.A. Henriksen, K. Takeuchi, O. Schaefer, B. Liu, J. ten Hoeve, Z. Ren, X. Mao, X. Chen, K. Shuai, and J.E. Darnell Jr. 2005. Implications of an antiparallel dimeric structure of nonphosphorylated STAT1 for the activation-inactivation cycle. *Proc. Natl. Acad. Sci. USA*. 102:3966–3971. doi:10.1073/pnas.0501063102



## Molecular mechanisms of the immunological abnormalities in hyper-IgE syndrome

Yoshiyuki Minegishi and Masako Saito

Department of Immune Regulation, Tokyo Medical and Dental University, Tokyo, Japan

Address for correspondence: Yoshiyuki Minegishi, 1-5-45 Yushima, Bunkyo-ku, Tokyo 113-8519, Japan.  
yminegishi.mbch@tmd.ac.jp

Hyper-IgE syndrome (HIES) is a primary immunodeficiency characterized by atopic dermatitis associated with extremely high serum IgE levels and susceptibility to staphylococcal skin abscesses and pneumonia. Recent studies have identified dominant negative mutations in the signal transducer and activator of transcription 3 gene (*STAT3*) as a major molecular cause of classical hyper-IgE syndrome, but the molecular mechanisms underlying this syndrome remain unclear. We recently showed that the impaired development of interleukin 17 (IL-17)–producing T helper cells (Th17 cells) due to defective IL-6 and IL-23 signaling in T cells, and the impaired generation of induced regulatory T (iT<sub>reg</sub>) cells from defective IL-10 signaling in dendritic cells, may account for the immunological abnormalities of hyper-IgE syndrome. These findings open up possibilities for exploring new approaches to the treatment of HIES patients.

**Keywords:** Th17 cell; iTreg cell; staphylococcal infection; atopic dermatitis; *STAT3*

### Introduction

Hyper-IgE syndrome (HIES) is a complex primary immunodeficiency disorder (PID) characterized by recurrent staphylococcal skin abscesses and pneumonia, atopic dermatitis, and extremely high serum IgE levels.<sup>1,2</sup> Recent studies have demonstrated the multisystem nature of HIES,<sup>3</sup> the signs of which are not restricted to the immune system, extend to skeletal and lung parenchymal abnormalities, such as osteoporosis, fracture with minor trauma, scoliosis, hyperextensive joints, retention of primary teeth, bronchiectasis, and pneumatocele. Dominant-negative mutations in *STAT3* have been identified as a major molecular cause of the multisystem HIES.<sup>4,5</sup> However, our understanding of the molecular mechanism underlying this syndrome remains limited. In this review, we focus on the molecular mechanisms underlying immunological manifestations of HIES due to dominant negative mutations in *STAT3*.

### STAT3

*STAT3* plays a critical role in signal transduction for many cytokines and growth factors, including those of the  $\gamma c$  family (IL-2, IL-4, IL-7, IL-9, IL-15,

IL-21), the gp130 family (IL-6, IL-11, IL-27, IL-31), the IL-10 family (IL-10, IL-19, IL-20, IL-22, IL-24, IL-26, IL-28, IL-29), and receptor-type tyrosine kinases (M-CSF, Flt-3, PDGF, EGF, FGF, GH, IGF) (Table 1).<sup>6</sup> *STAT3* functions as a transcription factor, binding to promoter regions and initiating transcription of its target genes. *STAT3* mediates signaling for about 40 cytokines and growth factors. It is, therefore, not straightforward to determine which pathway, in which cell type is critical for the signs of HIES. Studies of a null mutation of the *STAT3* gene in mice demonstrated that *STAT3* was essential for embryo survival close to the time of implantation (E6.5–E7.5).<sup>7</sup> Other studies of mice with a tissue-specific deletion of *STAT3* demonstrated the critical role of *STAT3* in cell survival, proliferation, migration, apoptosis, and inflammation in diverse cells including keratinocytes, hepatocytes, thymic epithelial cells, respiratory epithelial cells, neurons, lymphocytes, and macrophages.<sup>8</sup> The multisystem signs in HIES patients probably reflect the diverse functions *in vivo* of *STAT3* in humans.

### Th17 cells

Th17 cells—a subset of helper T cells producing cytokines including IL-17A, IL-17E, and IL-22—

**Table 1.** Ligands, receptors, and Jak family kinases upstream of STAT3

	Ligands		Receptors		Jak family kinases		
$\gamma$ c family	IL-2	$\gamma$ c	IL-2Ra	IL-2Rb	Jak1	Jak3	
	IL-4	$\gamma$ c	IL-4Ra		Jak1	Jak3	
	IL-7	$\gamma$ c	IL-7Ra		Jak1	Jak3	
	IL-9	$\gamma$ c	IL-9Ra		Jak1	Jak3	
	IL-15	$\gamma$ c	IL-15Ra	IL-2Rb	Jak1	Jak3	
	IL-21	$\gamma$ c	IL-21R		Jak1	Jak3	
IFNs	IFN- $\alpha$	IFNAR1	IFNAR2		Jak1	Tyk2	
	IFN- $\beta$	IFNAR1	IFNAR2		Jak1	Tyk2	
	IFN- $\gamma$	IFNGR1	IFNGR2		Jak1	Jak2	
IL-12/23	IL-12	IL-12Rb1	IL-12Rb2		Jak2	Tyk2	
	IL-23	IL-12Rb1	IL-23R		Jak2	Tyk2	
gp130 family	IL-6	gp130	IL-6Ra		Jak1	Jak2	Tyk2
	IL-11	gp130	IL-11Ra		Jak1	Jak2	Tyk2
	IL-27	gp130	IL-27Ra		Jak1	Jak3	
	IL-31	gp130	IL-31Ra		Jak1	Jak3	
	LIF	gp130	LIFR		Jak1	Jak3	
	OSM	gp130	OSMRb		Jak1	Jak3	
	CNTF	gp130	CNTFR		Jak1	Jak3	
	CT-1	gp130	CT-1R		Jak1	Jak3	
IL-10 family	IL-10	IL-10R2	IL-10R1		Jak1	Tyk2	
	IL-19	IL-20R1	IL-20R2		Jak1	Jak2	
	IL-20	IL-20R1	IL-20R2		Jak1	Jak2	
	IL-22	IL-10R2	IL-22R		Jak1	Tyk2	
	IL-24	IL-20R1	IL-20R2		Jak1	Jak2	
	IL-26	IL-10R2	IL-20R1		Jak1	Jak2	
	IL-28	IL-10R2	IL-28R1		Jak1	Tyk2	
	IL-29	IL-10R2	IL-28R1		Jak1	Tyk2	
Receptor type	M-CSF	M-CSFR			–		
	Flt3L	Flt3			–		
	PDGF	PDGFR			–		
	EGF	EGFR			–		
	FGF	FGFR			–		
	GH	GHR			–		
	IGF	IGFR			–		
Others	IL-5	$\beta$ c	IL-5Ra		Jak1	Jak2	
	G-CSF	G-CSFR			Jak1	Jak2	Tyk2
	Leptin	LEPR			Jak2		
	PAF	PAFR			Jak2		

have been extensively studied as inducers of auto-immune disorders.<sup>9–13</sup> Recent studies have also indicated that Th17 cells play a key role in host defense against extracellular bacteria and fungi.<sup>14,15</sup> Interestingly, most staphylococcal and *Candida* infections occurring in patients with HIES are

confined to the skin and lung, whereas in patients with chronic granulomatous disease—another human primary immunodeficiency—staphylococcal infections are frequently systemic.<sup>16</sup> These clinical observations suggest that Th17 cytokines play an important role in host defense on the

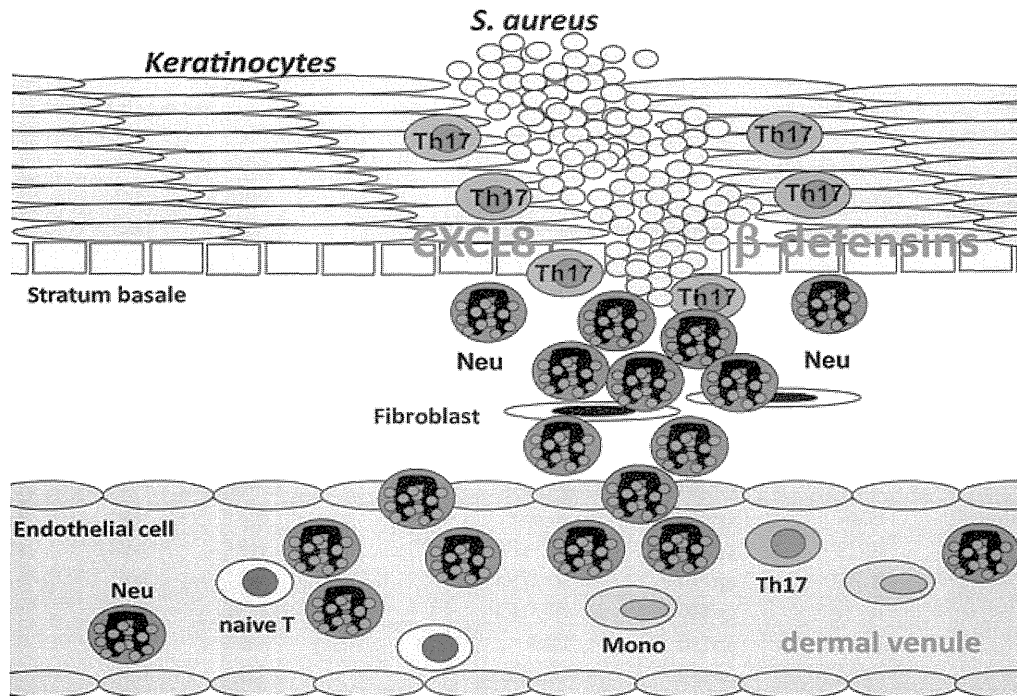


**Figure 1.** Protection against *Staphylococcus aureus* at the skin. The production of Th17 cytokines is severely decreased in HIES patients, which is required for the production of antimicrobial peptides, including  $\beta$ -defensin 2 and  $\beta$ -defensin 3, and neutrophil-recruiting chemokines, including CXCL8 (IL-8) from keratinocytes. The lack of antimicrobial peptides and neutrophil-recruiting chemokines may result in the susceptibility to staphylococcal infection in the skin.

surface of the body, particularly in the skin and airways.

Many reports have indicated that the production of Th17 cytokines, including IL-17A, IL-17E, and IL-22, by activated T cells from HIES patients is much lower than those from control individuals, whereas the production of other proinflammatory cytokines, including IFN- $\gamma$ , IL-1 $\beta$ , and TNF- $\alpha$ , is unaffected.<sup>17–21</sup> Such findings raise the questions of why and how systemic Th17 cell defects lead to staphylococcal infections restricted to the skin and lungs.

Insight into these questions was provided by the experimental observation that while supernatant from activated T cells from normal subjects induce keratinocyte and bronchial epithelial cell production of neutrophil-recruiting chemokines and  $\beta$ -defensins, supernatant from activated T cells from STAT3-deficient patients does not.<sup>21</sup> Human primary keratinocytes and bronchial epithelial cells do not produce sufficiently large amounts of neutrophil-recruiting chemokines and  $\beta$ -defensins in response to Th17 cytokines or classical proin-

flammatory cytokines.<sup>21</sup> Further support for these findings was provided by the demonstration *in vitro* that neutralization of Th17 cytokines decreases the production of the chemokines and defensins.<sup>21</sup> In contrast to those data, primary dermal fibroblasts and endothelial cells were found to respond equally well to T cell supernatants from HIES patients and controls. Thus, keratinocytes and bronchial epithelial cells respond differently from other types of cells (e.g., fibroblasts and endothelial cells) to Th17 cytokines, with Th17 cytokines playing a more important role in the production of chemokines and  $\beta$ -defensins in epithelial cells. One interpretation of this observation is that epithelial cells are always exposed to external stimuli and therefore have developed a system that is unresponsive to a single stimulation (such as Th17 cytokines) yet are responsive to combinations of stimulations. By contrast, internal cells, including fibroblasts and endothelial cells, must respond to single stimuli more rapidly because such first signals are often indicative of pathogen invasion, which requires an immediate response.

These previously published data<sup>21</sup> strongly indicate that Th17 cytokines play a crucial role in human host defense against *Staphylococcus aureus*, particularly at the surface barriers of the body (Fig. 1). Systemic T cell defects are converted into local defects, because only keratinocytes and bronchial epithelial cells require cytokines produced by Th17 cells in order to secrete neutrophil-recruiting chemokines and antimicrobial peptides. These findings provide at least a partial explanation for the restriction of staphylococcal infections to the skin and lungs of HIES patients and highlight the physiological role of Th17 cytokines in protection against extracellular pathogens in humans.<sup>21</sup>

### Induced regulatory T cells

One of the potential mechanisms of atopic dermatitis development in HIES is an acceleration of Th2 cell activity.<sup>22–24</sup> Effector Th2 cells are considered to be the major cell type that responds to allergens and produces Th2 cytokines, including IL-4, IL-5, IL-9, and IL-13. These Th2 cytokines induce changes in blood vessels, upregulate adhesion molecules, and recruit eosinophils. Th2 cytokines also induce class switching to IgE.<sup>25</sup> Recently identified cytokines such as IL-25, IL-31, and IL-33 also participate in Th2 cell-mediated inflammatory diseases.<sup>26–28</sup> In addition to Th2 cells, Th1 cells play a role in the pathogenesis of atopic dermatitis—contributing at a later time point—by inducing the apoptosis of epithelial cells.<sup>29</sup>

Another potential mechanism by which atopic dermatitis may develop in HIES patients is by impairment of regulatory T ( $T_{reg}$ ) cell activity;  $T_{reg}$  cells are key mediators of peripheral tolerance that suppress effector Th2 cells. The transcription factor Foxp3 is an important regulator of the development, function, and survival of  $T_{reg}$  cells, as clearly demonstrated by primary immunodeficiency in which patients lack FOXP3 gene expression and present with severe autoimmune and atopic phenotypes. Mutations in the human FOXP3 gene (*FOXP3*) result in immune dysregulation, polyendocrinopathy, enteropathy, and X-linked (IPEX) syndrome.<sup>30,31</sup> Foxp3 deficiency in mice also leads to atopic phenotypes.<sup>32,33</sup>

There are at least two types of Foxp3<sup>+</sup>  $T_{reg}$  cells: natural  $T_{reg}$  ( $nT_{reg}$ ) cells and induced  $T_{reg}$  ( $iT_{reg}$ ) cells. Natural  $T_{reg}$  cells develop in the thymus, whereas  $iT_{reg}$  cells develop in the periphery. TGF- $\beta$

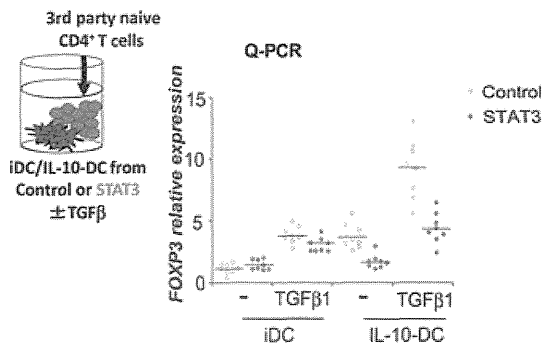


**Figure 2.** Q-PCR analysis of relative *FOXP3* mRNA expression (FOXP3/HPRT) after the co-culture of third-party allogeneic naive CD4<sup>+</sup> T cells from a control subject with untreated immature DCs (iDCs) or IL-10-DCs from eight controls and eight *STAT3* patients in the absence or presence of exogenous TGF- $\beta$ 1. IL-10-DCs upregulate *FOXP3* expression as efficiently as TGF- $\beta$ 1 and the combination of IL-10-DCs and TGF- $\beta$  synergistically upregulates the expression of *FOXP3*.

plays a crucial role in the induction of  $iT_{reg}$  cells; its expression in the presence of TCR stimulation converts naive Foxp3<sup>-</sup>CD4<sup>+</sup> T cells into Foxp3<sup>+</sup>  $iT_{reg}$  cells.<sup>34–37</sup> In addition to soluble factors, dendritic cells play a key role in the induction of  $T_{reg}$  cells.<sup>38,39</sup>

It has been shown that dendritic cells of patients with HIES display defective IL-10 signaling, which results in impaired suppression of cytokine production and T cell proliferation. In addition, dendritic cells from HIES patients are defective in generating Foxp3<sup>+</sup>  $iT_{reg}$  cells by IL-10 treatment.<sup>40</sup> Defective generation of  $iT_{reg}$  cells in response to IL-10 has also been observed in the other form of HIES that results from TYK2 deficiency.<sup>41</sup>

In terms of the molecular mechanisms involved, IL-10 normally upregulates the expression of PD-L1 and ILT-4 on the surface of dendritic cells, and both of these molecules are required for the induction of Foxp3<sup>+</sup>  $iT_{reg}$  cells.<sup>40</sup> In addition, IL-10-treated dendritic cells induce  $iT_{reg}$  cells as efficiently as does TGF- $\beta$ , and the combination of IL-10-treated dendritic cells and TGF- $\beta$  synergistically induces  $iT_{reg}$  cells (Fig. 2). Both of these IL-10-mediated pathways are likely defective in HIES patients. IL-10 signaling in dendritic cells is crucial for generating  $iT_{reg}$  cells *in vivo* and thus for maintaining an appropriate Th2– $T_{reg}$  cell balance to prevent hyper-IgE syndrome.